

Scaling and crossovers in activated escape near a bifurcation point

D. Ryvkine, M.I. Dykman, and B. Golding
Department of Physics and Astronomy, Michigan State University
(Dated: November 9, 2018)

Near a bifurcation point a system experiences critical slowing down. This leads to scaling behavior of fluctuations. We find that a periodically driven system may display three scaling regimes and scaling crossovers near a saddle-node bifurcation where a metastable state disappears. The rate of activated escape W scales with the driving field amplitude A as $\ln W \propto (A_c - A)^\xi$, where A_c is the bifurcational value of A . With increasing field frequency the critical exponent ξ changes from $\xi = 3/2$ for stationary systems to a dynamical value $\xi = 2$ and then again to $\xi = 3/2$. The analytical results are in agreement with the results of asymptotic calculations in the scaling region. Numerical calculations and simulations for a model system support the theory.

PACS numbers: 05.40.-a, 05.70.Ln, 77.80.Fm, 89.75.Da

I. INTRODUCTION

Thermally activated transitions are at root of many physical phenomena: diffusion in solids, protein folding, and nucleation are examples. It is important to understand how transitions occur, particularly in systems away from thermal equilibrium. Full understanding would include a description of the underlying dynamics and the transition probabilities. Owing to their exponential sensitivity, these probabilities provide an important means of characterizing a system. However, in many cases activation barriers are high which leads to very low transition rates and impedes precise experimental studies.

The barrier for escape from a metastable state is reduced when the system is close to a bifurcation (critical, or spinodal) point where the state disappears. For systems that display hysteresis such a bifurcation point corresponds to the switching point on the hysteresis loop. The idea of bringing the system close to the bifurcation point [1] has been used in studying activated switching in Josephson junctions [2, 3, 4, 5], where it has become a standard technique for determining the critical current. This idea is also used in studies of activated magnetization reversals in nanomagnets [6, 7, 8].

Experiments on nanomagnets and Josephson junctions are often performed by ramping the control parameter (magnetic field or current) and measuring time distribution of escape events [1]. In interpreting the data it is usually assumed that, for sufficiently slow ramp rates, the system remains quasistationary. In this approximation the barrier height, i.e., the activation energy of a transition R , usually scales with the control parameter η , measured from its critical (bifurcational) value $\eta_c = 0$, as $\eta^{3/2}$ [9, 10].

Scaling of R near a bifurcation point is related to slowing down of one of the motions [11], i.e., the onset of a “soft mode”. The relaxation time of the system t_r diverges as the control parameter $\eta \rightarrow 0$. Therefore if η depends on time, even where this dependence is slow the assumption of quasistationary may become inapplicable for small η .

In this paper a theory of activated transitions is devel-

oped for periodically modulated systems. In such systems the notion of a stable state is well-defined irrespective of the modulation rate, and the applicability of the quasistationary approximation can be carefully studied. It turns out that, unexpectedly, near a critical point this approximation breaks down even where the relaxation time t_r is still much smaller than the driving period $\tau_F = 2\pi/\omega_F$.

We show that an interplay between the critical slowing down and the slowness of time-dependent modulation leads to a rich scaling behavior of the transition rate and to crossovers between different scaling regions. This behavior near a bifurcation point is system-independent and has no counterparts in stationary systems. We find three regions in which the activation energy scales as $R \propto \eta^\xi$. As the parameters change, for example with the increase of the modulation frequency ω_F , the critical exponent ξ varies from $3/2$ to 2 and then again to $3/2$. Our numerical calculations and Monte Carlo simulations for a model system agree with the general results.

Activated transitions in periodically driven systems were investigated earlier in various contexts [12, 13, 14, 15, 16, 17, 18, 19, 20], stochastic resonance and diffusion in modulated ratchets being recent examples [21, 22, 23]. In this paper we study the previously unexplored region of driving amplitudes close to critical and reveal the universality that emerges.

A qualitative picture of motion near a bifurcation point can be obtained if one thinks of the system as a particle in a potential $U(q, t)$ that oscillates in time with period τ_F , see Fig. 1. Such particle has periodic stable and unstable states, $q_a(t)$ and $q_b(t)$. In the adiabatic limit $\omega_F \rightarrow 0$ they lie at the minimum and local maximum of the potential in Fig. 1a. As the modulation amplitude A increases, the states become close to each other for a portion of the period τ_F , see Fig. 1b. The barrier height reaches its minimum during this time, and this is when the system is most likely to escape from the potential well.

As A further increases, the states $q_{a,b}(t)$ become distorted to avoid crossing, see Fig. 1c, and the adiabatic approximation becomes inapplicable. The parameter range

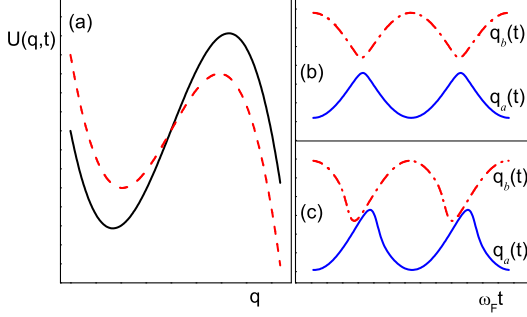


FIG. 1: (a) An oscillating potential barrier. In the limit of slow modulation, the stable and unstable periodic states q_a and q_b are the instantaneous positions of the potential minimum and barrier top, respectively. (b) For slow modulation, when the driving amplitude A is close to A_c^{ad} , the states $q_{a,b}(t)$ come close to each other once per period. (c) As A further approaches A_c , the states $q_{a,b}(t)$ become skewed compared to the adiabatic picture, to avoid crossing. In the critical range, the form of $q_{a,b}(t)$ is model-independent.

where it happens can be estimated by noticing that the adiabatic relaxation time t_r (i) is a function of the instantaneous modulation phase $\phi = \omega_F t$, and (ii) sharply increases near the bifurcation point. As a consequence, t_r sharply increases when ϕ approaches the value where $q_{a,b}$ are at their closest, because this corresponds to approaching the bifurcation point. The quasistationary (adiabatic) approximation requires that $|\partial t_r / \partial t| \ll 1$. It is this condition that limits the range of adiabaticity, rather than a much less restrictive condition $t_r \omega_F \ll 1$.

Even for $A > A_c^{\text{ad}}$, where the adiabatic barrier in Fig. 1 disappears for a portion of the period, the states $q_{a,b}$ may still coexist. A sufficiently large fluctuation is then required to move the system away from the stable periodic state. It is in this region that the new scaling of the activation energy R emerges. The control parameter is now $\eta \propto A_c - A$, where A_c is the “true” bifurcation value of the modulation amplitude.

In the limit $\omega_F t_r \gg 1$ the behavior near a bifurcation point is in some sense simpler. In this case $q_a(t)$ and $q_b(t)$ come close to each other everywhere on the cycle, not just for a part of the period. The motion of the system in the vicinity of $q_{a,b}(t)$ is oscillations about the state $q_a(t)$ with a slowly varying amplitude. The amplitude change can be described by averaging the complete dynamics over the period. It is then mapped onto motion in an effectively stationary potential. Not surprisingly, the scaling of the escape activation energy R with the distance to the bifurcation point is the same as for stationary systems.

In Sec. II and Appendix A we provide a general formulation of the problem of activated escape in periodically modulated systems driven by Gaussian noise. In Sec. III A and Appendix B we discuss the dynamics near a bifurcation point in the adiabatic limit $\omega_F t_r \rightarrow 0$. In Sec. III B we consider the strongly nonadiabatic dynam-

ics that emerges where still $\omega_F t_r \ll 1$. In Sec. III C and Appendix C the dynamics near a bifurcation point is described in the parameter range where the field becomes effectively fast-oscillating, i.e. $\omega_F t_r \gg 1$, even though the relaxation time in the absence of modulation $t_r^{(0)}$ may be $\lesssim 1/\omega_F$. The connection between the nonadiabatic local theory of Sec. III B and the theory of Sec. III C is discussed in Sec. III D. In Sec. IV the activation energy is explicitly evaluated in the three regions discussed in Sec. III, and the scaling laws for the activation energy $R \propto (A_c - A)^\xi$ in these regions are obtained. The scaling crossovers are discussed. We also find nonadiabatic corrections to the escape rate in the adiabatic region. In Sec. V we consider a periodically modulated Brownian particle. Numerical results for the activation energy are compared to the results of Monte Carlo simulations and to the predictions of Sec. IV. Sec. VI contains concluding remarks.

II. ACTIVATED ESCAPE: GENERAL FORMULATION

We will adopt a phenomenological approach in which a multidimensional system with dynamical variables $\mathbf{q}(t)$ is described by the Langevin equation

$$\dot{\mathbf{q}} = \mathbf{K}(\mathbf{q}; A, t) + \mathbf{f}(t), \quad \mathbf{K}(\mathbf{q}; A, t + \tau_F) = \mathbf{K}(\mathbf{q}; A, t). \quad (1)$$

The function \mathbf{K} is periodic in time, with the modulation period $\tau_F = 2\pi/\omega_F$; A is a control parameter that characterizes the modulation strength. For example, in the case of an overdamped particle in a potential $U_0(\mathbf{q})$ modulated by an additive periodic force $\mathbf{F}(t)$, the vector \mathbf{K} becomes

$$\mathbf{K}(\mathbf{q}; A, t) = -\nabla U_0(\mathbf{q}) + \mathbf{F}(t). \quad (2)$$

(here and below, $\nabla \equiv \partial/\partial\mathbf{q}$). In this case $A = \max|\mathbf{F}|$ is the modulation amplitude (note that the force $\mathbf{F}(t) = \mathbf{F}(t + \tau_F)$ does not have to be sinusoidal).

The function $\mathbf{f}(t)$ in Eq. (1) is zero-mean Gaussian noise with correlation matrix

$$\varphi_{ij}(t - t') = \langle f_i(t) f_j(t') \rangle. \quad (3)$$

The characteristic noise intensity D can be defined as the maximal value of the power spectrum,

$$D = \max \Phi_{nn}(\omega), \quad \Phi_{nm}(\omega) = \int dt e^{i\omega t} \varphi_{nm}(t). \quad (4)$$

For thermal fluctuations $D = 2k_B T$. The noise intensity D is the smallest parameter of the theory. Smallness of D leads to the rate of noise-induced escape W being much smaller than t_r^{-1} and ω_F .

In the absence of noise, Eq. (1) may have different periodic solutions \mathbf{q}_{per} , which can be stable (attractors), unstable (repellers), or hyperbolic (saddles). We are interested in the parameter range where one of the stable

periodic solutions $\mathbf{q}_a(t) = \mathbf{q}_a(t + \tau_F)$ comes close to a saddle-type periodic solution $\mathbf{q}_b(t)$ with the same period (period 1, for concreteness). For slow modulation, these states are sketched in Fig. 1. They merge together at the saddle-node bifurcation point $A = A_c$. In what follows we will assume that A is close to the critical value A_c .

Escape from a metastable state $\mathbf{q}_a(t)$ occurs as a result of a large fluctuation. The fluctuational force $\mathbf{f}(t)$ has to overcome the restoring force \mathbf{K} and drive the system away from the basin of attraction to $\mathbf{q}_a(t)$ [e.g., away from the potential well in Fig. 1]. We will assume that the required force $\mathbf{f}(t)$ is much larger than the typical noise amplitude $\propto D^{1/2}$.

The motion of the system during escape is random. However, different trajectories have exponentially different probabilities. The system is most likely to move along a particular trajectory called the optimal path $\mathbf{q}_{\text{opt}}(t)$ [24]. It is determined by the most probable noise realization $\mathbf{f}_{\text{opt}}(t)$. In the case of a periodically modulated 1D system driven by stationary Gaussian noise, a way to find the optimal paths was discussed earlier [18]. We now briefly outline a generalization of the formulation to multidimensional systems, following the arguments in Ref. 25 (more details are provided in Appendix A).

For a stationary Gaussian noise, the probability density of realizations of $\mathbf{f}(t)$ is given by the functional (cf. Ref. 26)

$$\mathcal{P}[\mathbf{f}(t)] = \exp(-\mathcal{R}_0[\mathbf{f}(t)]/D), \quad (5)$$

where \mathcal{R}_0 is quadratic in \mathbf{f} ,

$$\mathcal{R}_0[\mathbf{f}] = \frac{1}{2} \iint dt dt' f_i(t) \mathcal{F}_{ij}(t - t') f_j(t'). \quad (6)$$

The matrix \mathcal{F} is the inverse of $\varphi_{ij}(t - t')/D$,

$$\int dt' \mathcal{F}_{ij}(t - t') \varphi_{jk}(t' - t'') = D \delta_{ik} \delta(t - t''). \quad (7)$$

We are interested in noise realizations that lead to escape, and therefore $\mathbf{f}(t)$ largely exceeds its root-mean-square value. From Eq. (5), the probabilities of such noise realizations are exponentially small and exponentially strongly depend on the form of $\mathbf{f}(t)$. As a consequence, escape trajectories should form a narrow "tube" centered at an optimal path $\mathbf{f}_{\text{opt}}(t)$ that maximizes $\mathcal{P}[\mathbf{f}(t)]$, i.e., minimizes $\mathcal{R}_0[\mathbf{f}(t)]$. The minimum of \mathcal{R}_0 should be found with the constraints that (i) the system and noise trajectories, $\mathbf{q}_{\text{opt}}(t)$ and $\mathbf{f}_{\text{opt}}(t)$, are interrelated by the equation of motion (1), (ii) the path $\mathbf{q}_{\text{opt}}(t)$ starts in the vicinity of the stable state $\mathbf{q}_a(t)$ and ends behind or on the boundary of the basin of attraction to $\mathbf{q}_a(t)$, and (iii) the force $\mathbf{f}_{\text{opt}}(t)$ is equal to zero before the escape event happens and becomes equal to zero once the system has escaped, so that, as $\mathbf{f}_{\text{opt}}(t)$ decays, it does not drag the system back to the basin of attraction to \mathbf{q}_a .

As explained in Appendix A, these conditions lead to boundary conditions for optimal paths of the form

$$\mathbf{q}_{\text{opt}}(t) \rightarrow \begin{cases} \mathbf{q}_a(t) & \text{for } t \rightarrow -\infty, \\ \mathbf{q}_b(t) & \text{for } t \rightarrow \infty, \end{cases}$$

$$\mathbf{f}_{\text{opt}}(t) \rightarrow 0 \text{ for } t \rightarrow \pm\infty \quad (8)$$

(note that $\mathbf{q}_{\text{opt}}(t)$ ends on the basin boundary, not on another attractor.)

The variational problem for optimal paths is reduced to minimizing the functional

$$\begin{aligned} \mathcal{R}[\mathbf{q}, \mathbf{f}] = & \mathcal{R}_0[\mathbf{f}] \\ & + \int dt' \boldsymbol{\lambda}(t') \cdot [\dot{\mathbf{q}}(t') - \mathbf{K}(\mathbf{q}; A, t') - \mathbf{f}(t')] \end{aligned} \quad (9)$$

with boundary conditions (8). The function $\boldsymbol{\lambda}(t)$ is a Lagrange multiplier. The boundary condition for it follows from the fact that the system only needs to be driven by a large force $\mathbf{f}(t)$ when it moves from the attractor to the basin boundary. Therefore $\boldsymbol{\lambda}(t) \rightarrow 0$ for $t \rightarrow \pm\infty$.

It follows from Eqs. (8), (9) and from the results of Appendix A that the optimal trajectories $\mathbf{q}_{\text{opt}}(t), \mathbf{f}_{\text{opt}}(t)$ are instanton-like [27]. The typical duration of motion is given by the relaxation time of the system t_r and the noise correlation time t_{corr} . In stationary systems instantons are translationally invariant with respect to time, i.e., if $\mathbf{q}_{\text{opt}}(t), \mathbf{f}_{\text{opt}}(t)$ is a solution, then $\mathbf{q}_{\text{opt}}(t + \tau), \mathbf{f}_{\text{opt}}(t + \tau)$ is also a solution, for an arbitrary τ . In contrast, in periodically modulated systems this is true only for $\tau = \tau_F$. The instantons are synchronized by the modulation: generally there is one instanton per period that would provide a global minimum to \mathcal{R} .

From Eq. (5), we obtain for the escape probability

$$W \propto \exp(-R/D), \quad R = \min \mathcal{R}[\mathbf{q}, \mathbf{f}]. \quad (10)$$

The activation energy R is equal to the functional $\mathcal{R}_0[\mathbf{f}_{\text{opt}}]$ calculated for the optimal noise trajectory for escape.

For small noise intensity, the escape rate $W \ll \omega_F$. It periodically depends on time. However, in the small- D limit this dependence is seen only in the prefactor [15, 16, 17]. Here we are interested in the exponent, which gives the period-averaged escape rate \bar{W} . It is equal to the probability of escape over the time τ_F divided by τ_F

In the general case, the variational problem for the activation energy can be solved only numerically. Therefore it is particularly important to find model-independent properties of R . So far they have been found for comparatively weak modulation, where it was shown that R has a term linear in the modulation amplitude [18]. In this paper we analyze the activation energy R in a previously unexplored region near a bifurcation point and show that R displays a nontrivial scaling behavior in this region.

III. DYNAMICS NEAR A BIFURCATION POINT

The dynamics near a saddle-node bifurcation point has universal features related to the occurrence of a slow variable, or a "soft mode" [11]. For periodically modulated systems, closeness to the bifurcation point in the parameter space usually implies that the merging states are close

to each other in phase space throughout the modulation period.

If the modulation frequency ω_F is small compared to the reciprocal relaxation time in the absence of modulation $1/t_r^{(0)}$, there emerges a situation where the stable and unstable states come close to each other only for a portion of a period. During this time, the system behaves as if it were close to a true bifurcation point. Then it is possible to single out a slow variable that controls the system dynamics. Escape from a metastable state is most probable when $\mathbf{q}_a(t)$ and $\mathbf{q}_b(t)$ are closest to each other.

On the other hand, if the modulation frequency $\omega_F \gtrsim 1/t_r^{(0)}$, near the bifurcation point the states $\mathbf{q}_a(t)$ and $\mathbf{q}_b(t)$ are close to each other throughout the modulation period. Then escape events should be no longer synchronized by the modulation.

Because the dynamics near a bifurcation point is slow, the system filters out high-frequency components of the noise. As a result, the noise becomes effectively δ -correlated (we will not consider here the situation where the noise power spectrum has singular features at high frequencies). The reduction to one slow variable driven by white noise can be done directly in the equations of motion. For slow modulation ($\omega_F t_r^{(0)} \ll 1$), this reduction is local in time (see Appendix B), otherwise it has to be done globally over the cycle (see Appendix C). Alternatively, the dimensionality reduction can be done directly in the variational problem for the optimal escape path (see Appendix A).

A. The adiabatic approximation

In the limit of slow modulation, where the period of the field τ_F is large compared to the system relaxation time $t_r^{(0)}$, a convenient starting point of the analysis is the adiabatic approximation. The adiabatic periodic states of the system $\mathbf{q}_{\text{per}}^{\text{ad}}$ are given by the equation

$$\mathbf{K}(\mathbf{q}_{\text{per}}^{\text{ad}}; A, t) = 0, \quad (11)$$

which is obtained by disregarding $\dot{\mathbf{q}}$ and the noise \mathbf{f} in the equation of motion (1).

The adiabatic stable state (attractor) $\mathbf{q}_a^{\text{ad}} \equiv \mathbf{q}_a^{\text{ad}}(t)$ is the solution $\mathbf{q}_{\text{per}}^{\text{ad}}$ for which the real parts of the eigenvalues of the matrix $\hat{\mu} = (\partial K_i / \partial q_j)$ are all negative. These eigenvalues give the “instantaneous” relaxation rates, for a given phase of the modulation $\phi = \omega_F t$. For the periodic adiabatic saddle-type state $\mathbf{q}_b^{\text{ad}}(t)$ one of the eigenvalues of $\hat{\mu}$ has a positive real part.

In the adiabatic approximation, the saddle-node bifurcation occurs in the following way. At the critical value of the control parameter $A = A_c^{\text{ad}}$, the periodic trajectories $\mathbf{q}_a^{\text{ad}}(t)$ and $\mathbf{q}_b^{\text{ad}}(t)$ given by (11) merge, but it happens only once per period. One can picture it by looking at Fig. 1 (b) and imagining that the states $\mathbf{q}_a(t)$ and $\mathbf{q}_b(t)$ touch each other. We set the corresponding instant

of time equal to $t = 0$ (or $t = n\tau_F$), i.e., we assume that $\mathbf{q}_a^{\text{ad}}(0) = \mathbf{q}_b^{\text{ad}}(0)$ for $A = A_c^{\text{ad}}$. Additionally, we set $\mathbf{q}_a^{\text{ad}}(0) = \mathbf{q}_b^{\text{ad}}(0) = \mathbf{0}$.

At the adiabatic bifurcation point $A = A_c^{\text{ad}}, t = 0$ one of the eigenvalues μ_1 of the matrix $\hat{\mu}$ is equal to zero, whereas all other eigenvalues $\mu_{i>1}$ have *negative* real parts. The adiabatic approximation means that $\text{Re } \mu_{i>1} \gg \omega_F$, or equivalently, that the relaxation time $\max |\text{Re } \mu_{i>1}|^{-1}$ is small compared to τ_F . This relaxation time is typically of the order of $t_r^{(0)}$.

We now write the dynamical variables \mathbf{q} in the basis of the right eigenvectors of the matrix $\hat{\mu}$ at the bifurcation point and expand \mathbf{K} in the equation of motion (1) near the bifurcation point $\mathbf{q} = \mathbf{0}, t = 0, A = A_c^{\text{ad}}$. As shown in Appendix B, the motion described by the variable q_1 is much slower than the motion described by the variables $q_{i>1}$. Over the time $\sim t_r^{(0)}$ they “adjust” to the value of q_1 , i.e., they follow q_1 adiabatically. The variable q_1 is the soft mode. It satisfies the equation of motion

$$\begin{aligned} \dot{q}_1 &= K(q_1; A, t) + f_1(t), \\ K &= \alpha q_1^2 + \beta \delta A^{\text{ad}} - \alpha \gamma^2 (\omega_F t)^2. \end{aligned} \quad (12)$$

Here $\delta A^{\text{ad}} = A - A_c^{\text{ad}}$; the parameters α, β, γ are expressed in terms of the derivatives of \mathbf{K} at the adiabatic bifurcation point and are given by Eqs. (B3), (B4).

The stable and unstable adiabatic periodic states in the absence of noise exist for $\alpha \beta \delta A^{\text{ad}} < 0$. For concreteness and without loss of generality we set $\alpha > 0$. For small $|\omega_F t|$ the adiabatic states can be found by setting $K((q_1)_{a,b}^{\text{ad}}; A, t) = 0$. This gives

$$(q_1)_{a,b}^{\text{ad}} = \mp (2\alpha t_r^{\text{ad}})^{-1},$$

where t_r^{ad} is the instantaneous adiabatic relaxation time. It is given by $|\partial K / \partial q_1|^{-1}$ evaluated for $q_1 = (q_1)_a^{\text{ad}}$,

$$t_r^{\text{ad}} = \frac{1}{2} \left[-\alpha \beta \delta A^{\text{ad}} + (\alpha \gamma \omega_F t)^2 \right]^{-1/2} \quad (13)$$

[the explicit expression for $(q_1)_{a,b}^{\text{ad}}(t)$ is given by Eq. (B5)].

The applicability of the adiabatic approximation requires not only that $\omega_F t_r^{\text{ad}} \ll 1$, but also $|\partial t_r^{\text{ad}} / \partial t| \ll 1$, otherwise the system cannot follow the modulation. From Eq. (13), near the bifurcation point the time dependence of t_r^{ad} is pronounced, so that

$$\max |\partial t_r^{\text{ad}} / \partial t| = 3^{-3/2} \gamma \omega_F / |\beta \delta A^{\text{ad}}| \gg \omega_F t_r^{\text{ad}}.$$

Therefore the inequality $|\partial t_r^{\text{ad}} / \partial t| \ll 1$ is much stronger than $\omega_F t_r^{\text{ad}} \ll 1$. It holds if

$$t_r^{\text{ad}} \ll t_l, \quad t_l = (\alpha \gamma \omega_F)^{-1/2}, \quad (14)$$

i.e., $\omega_F \ll |\beta \delta A^{\text{ad}}| / \gamma$. The time t_l sets a new dynamical time scale that restricts the range of validity of the adiabatic approximation. It imposes an upper bound on the relaxation time of a periodically driven system where this approximation still applies.

B. Locally nonadiabatic regime

As A approaches A_c^{ad} , the criterion (14) is violated. The periodic stable and unstable states are pressed against each other. Since they cannot cross, they become distorted, as shown in Fig. 1c. Ultimately they merge, but along a line rather than at a point. From Eq. (12) one can see that this is just a straight line, which is described by the equation

$$q_{1c}(t) = \gamma\omega_F t. \quad (15)$$

Eqs. (12), (15) define the new nonadiabatic bifurcational value of the modulation amplitude for slow driving,

$$A_c^{\text{sl}} = A_c^{\text{ad}} + \beta^{-1}\gamma\omega_F. \quad (16)$$

The corrections to A_c^{sl} of higher order in ω_F are discussed in Sec. III C and obtained explicitly in Sec. V.

It is convenient to change in Eq. (12) to dimensionless variables $Q = \alpha t_l q_1$ and $\tau = t/t_l$, and to introduce the control parameter

$$\eta = \beta(\gamma\omega_F)^{-1}(A_c^{\text{sl}} - A). \quad (17)$$

This is the only parameter of a slowly driven system. It describes both adiabatic and nonadiabatic behavior and gives the reduced distance to the bifurcation point.

The equation of motion for the reduced variable takes the form

$$\frac{dQ}{d\tau} = G(Q, \eta, \tau) + \tilde{f}(\tau), \quad G = Q^2 - \tau^2 + 1 - \eta. \quad (18)$$

The function $\tilde{f}(\tau) = (\gamma\omega_F)^{-1}f_1(t)$ in Eq. (18) describes reduced noise. It is effectively δ -correlated on the slow-time scale, $\langle \tilde{f}(\tau)\tilde{f}(\tau') \rangle = 2\tilde{D}\delta(\tau - \tau')$, as explained in Appendix B. The noise intensity \tilde{D} is given by Eq. (B7).

The stable and unstable states $Q_{a,b}(\tau)$ are given by the equation $dQ/d\tau = G$. In the absence of noise this equation has symmetry $Q \rightarrow -Q, \tau \rightarrow -\tau$. As a consequence, the stable and unstable states are antisymmetric, $Q_b(\tau) = -Q_a(-\tau)$. Therefore it suffices to find only $Q_a(\tau)$.

We start with the adiabatic approximation. It applies for $\eta \gg 1$. The adiabatic stable and unstable states in the reduced variables are given by the equation $G = 0$ and have the form

$$Q_{a,b}^{\text{ad}} = \mp [\tau^2 + (\eta - 1)^2]^{1/2}. \quad (19)$$

Each of these states is symmetric with respect to $\tau = 0$, where they are closest to each other. The adiabatic bifurcation point is $\eta = 1$, which corresponds to $A = A_c^{\text{ad}}$.

The region $\eta \lesssim 1$ is nonadiabatic, and $\eta = 0$ (or $A = A_c^{\text{sl}}$) is the nonadiabatic bifurcation point for slow driving. At this point $Q_{a,b}(\tau)$ merge into the straight line $Q_c(\tau) = \tau$.

Close to the nonadiabatic bifurcation point, where $\eta \ll 1$, one can find $Q_{a,b}(\tau)$ by perturbation theory in the whole range $-\infty < \tau < |\ln \eta|^{1/2}/2$. The linearized equation for the difference $\delta Q(\tau) = Q_a(\tau) - \tau$ has a simple form $\frac{d\delta Q}{d\tau} = 2\tau \delta Q + \eta$. By solving it we obtain

$$Q_a(\tau) = -Q_b(-\tau) \approx \tau - \eta \int_{-\infty}^{\tau} d\tau_1 e^{\tau^2 - \tau_1^2}. \quad (20)$$

In the region of large negative τ the function $Q_a(\tau) = -Q_b(-\tau)$ has a simple form $Q_a(\tau) \approx -\tau - \eta(2\tau)^{-1}$. The states Q_a and Q_b are closest to each other, with separation $\sim \eta$, in the range $|\tau| < |\ln \eta|^{1/2}/2$. The interstate separation decreases as η approaches the bifurcational value $\eta = 0$. At the same time, the range of τ where Q_a and Q_b are close to each other increases with decreasing η .

As τ increases beyond $\approx |\ln \eta|^{1/2}/2$, there occurs a sharp crossover from the nearly linear in τ solution for $Q_a(\tau)$ (20) to the adiabatic solution (19) $Q_a \propto -\tau$. The functions $Q_{a,b}(\tau)$ for a specific value of η are shown in Fig. 2.

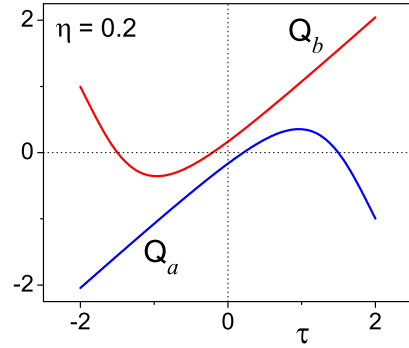


FIG. 2: Nonadiabatic stable and unstable states $Q_a(\tau)$ and $Q_b(\tau) = -Q_a(-\tau)$ for slow modulation as given by the equation $dQ/d\tau = G(Q, \eta, \tau)$ for $\eta = 0.2$. The functions $Q_{a,b}(\tau)$ are strongly asymmetric, in contrast to the adiabatic states (19) which are even functions of τ .

The interval of the real time $|t| \lesssim t_r = t_l |\ln \eta|^{1/2}$, where the states $Q_{a,b}$ are nearly linear in t , should be much smaller than $1/\omega_F$ in order for Eq. (12) to apply. This imposes a restriction on η ,

$$\eta \gg \exp(-C|\alpha|\gamma/\omega_F), \quad C \sim 1. \quad (21)$$

For smaller $\eta \propto |A_c^{\text{sl}} - A|$ the local approximation, where the coefficients are expanded about the adiabatic bifurcation point, no longer applies. The relaxation time t_r becomes comparable to the modulation period. It follows from Eq. (21), however, that for low frequencies the local approximation is extremely good.

On the whole, the locally nonadiabatic regime is limited in η by the condition $\eta \lesssim 1$ and by Eq. (21). The width of the amplitude range $A_c^{\text{sl}} - A$ imposed by the first

condition linearly increases with the field frequency, in the approximation (16). Therefore locally-nonadiabatic critical behavior is more pronounced for higher frequencies. However, the appropriate frequency range is limited from above by the condition (21). For higher ω_F there should occur a crossover to a fully nonlocal picture, which is discussed in the next section.

C. Fast-oscillating field

Sufficiently close to the "true" critical value of the modulation amplitude A_c , the relaxation time of the system becomes large compared to the modulation period even if $\omega_F t_r^{(0)} \lesssim 1$ far from the bifurcation point. The inequality $\omega_F t_r \gg 1$ defines the third region, in addition to the adiabatic and locally nonadiabatic, where we have analyzed the dynamics near a bifurcation point. The analysis of this region is simplified by the fact that here the modulating field is effectively fast-oscillating.

For $\omega_F t_r \gg 1$, near the bifurcation point the periodic stable and unstable states $\mathbf{q}_a(t)$ and $\mathbf{q}_b(t)$ stay close to each other throughout the cycle, see Fig. 3. For $A = A_c$, they coalesce into a periodic critical cycle $\mathbf{q}_c(t) = \mathbf{q}_c(t + \tau_F)$. When A is close to A_c and \mathbf{q} is close to \mathbf{q}_c , we can simplify the equations of motion (1) by expanding the function \mathbf{K} in $\delta\mathbf{q} = \mathbf{q} - \mathbf{q}_c$ and $\delta A = A - A_c$ (cf. Ref. 11),

$$\delta\dot{\mathbf{q}} = \hat{\mu}\delta\mathbf{q} + \frac{1}{2}(\delta\mathbf{q} \cdot \nabla)^2 \mathbf{K} + \delta A \frac{\partial}{\partial A} \mathbf{K} + \mathbf{f}(t). \quad (22)$$

Here $\mu_{ij} \equiv \mu_{ij}(t) = \partial K_i / \partial q_j$. All derivatives of \mathbf{K} are now evaluated for $A = A_c$ and $\mathbf{q} = \mathbf{q}_c(t)$. Therefore all coefficients in Eq. (22) are periodic functions of time.

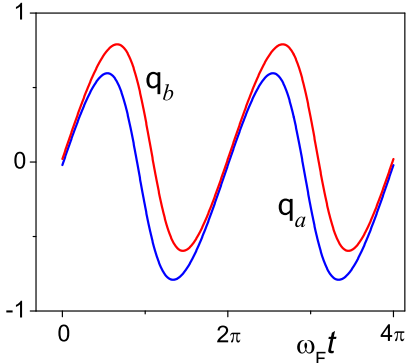


FIG. 3: The stable and unstable states, $\mathbf{q}_a(t)$ and $\mathbf{q}_b(t)$, close to the bifurcation point. For $\omega_F t_r \gg 1$ the states are close to each other throughout the modulation period. The figure refers to a one-dimensional overdamped particle in a potential $U(q, t) = \frac{1}{4}q - \frac{1}{3}q^3 - Aq \cos(\omega_F t)$ for $(A_c - A)/A_c \approx 0.01$. The modulation is comparatively slow, $\omega_F t_r^{(0)} = 1$, but for chosen A the relaxation time becomes long, $\omega_F t_r \approx 9.8$.

If initially the system is close to $\mathbf{q}_c(t)$, its distance from

$\mathbf{q}_c(t)$ will oscillate with frequency ω_F and with an amplitude that slowly varies over the period τ_F . This amplitude is a slow variable, $Q^{\text{sm}}(t)$. The equation for $Q^{\text{sm}}(t)$ can be obtained by an appropriate averaging method explained in Appendix C. After rescaling to dimensionless coordinate $Q \propto Q^{\text{sm}}$ and time $\tau \propto t$, see Eq. (C11), this equation takes a form which is similar to Eq. (18),

$$\begin{aligned} \frac{dQ}{d\tau} &= G(Q, \eta) + \tilde{f}(\tau), \\ G &= Q^2 - \eta, \quad \eta = \beta'(A_c - A) \end{aligned} \quad (23)$$

[in contrast to Eq. (18), the function G here is independent of time]. The coefficient β' is given by Eq. (C7).

The parameter η in Eq. (23) is the scaled distance to the bifurcation point. The stationary states $Q_{a,b} = \mp\eta^{1/2}$ exist for $\eta > 0$. They merge for $\eta = 0$. The noise $\tilde{f}(\tau)$ is effectively white on the time scale that largely exceeds ω_F^{-1} and the noise correlation time t_{corr} . Its intensity \tilde{D} is given by Eq. (C12).

The results of this Section and Appendix C refer to the case $\omega_F t_r \gg 1$, but arbitrary $\omega_F t_r^{(0)}$. Therefore the problem is different from the standard problem of slow motion in a fast-oscillating field [28], where of interest is the smooth term in the oscillating coordinate. In contrast, here we are interested in the slowly varying oscillation amplitude. If $\omega_F t_r^{(0)} \gg 1$, a transition to slow and fast variables can be made already in the original equation of motion (1), by separating \mathbf{q} into slow and fast oscillating parts. The equation for the slow part near the bifurcation point will again have the form (23), but the expressions (C7) for α', β' will be simplified [in particular, the factor κ_{11} in Eq. (C7) will be equal to one].

D. Connection to the locally nonadiabatic regime

Eq. (22) allows us to look from a different perspective at the locally nonadiabatic regime that emerges for $\omega_F t_r \ll 1$. In contrast to the approach of Sec. III B, where the starting point was the adiabatic approximation, here we will assume that A is close to the true bifurcational value of the amplitude A_c and that $\mathbf{q}(t)$ is close to the critical cycle $\mathbf{q}_c(t)$, at least for a part of the period τ_F .

For $\omega_F t_r \ll 1$, one can think of a local in time description of the dynamics near the cycle $\mathbf{q}_c(t)$. From Eq. (22), this dynamics is determined by the eigenvalues $\mu_\nu(t)$ of the matrix $\hat{\mu}(t)$. In contrast to the analysis of Sec. III A, we consider here the matrix $\hat{\mu}$ calculated for the critical cycle $\mathbf{q}_c(t)$ rather than the two similar matrices calculated separately for the adiabatic stable and unstable states.

For much of the driving period the real parts of $\mu_\nu(t)$ are all large, $|\text{Re } \mu_\nu| \sim 1/t_r^{(0)} \gg \omega_F$. Then, when the system is in the stable state, it follows the field adiabatically. The adiabaticity is broken where one of the eigenvalues, say $\mu_1(t)$, goes through zero. As we will see,

at this time the stable and unstable states are most close to each other. We set the time when it happens equal to zero, i.e., $\mu_1(0) = 0$.

For small $|t| \ll \tau_F$ the analysis of the system dynamics is in many respects similar to that in Sec. III B and Appendix C. First, $\delta\mathbf{q}(t)$ in Eq. (22) is written as $\sum_\nu \delta q_\nu \mathbf{e}_\nu(0)$, where $\mathbf{e}_\nu(0)$ are the right eigenvectors of the matrix $\hat{\mu}(0)$. The component δq_1 of $\delta\mathbf{q}$ along the eigenvector $\mathbf{e}_1(0)$ of $\hat{\mu}(0)$ will be the slow variable, or the soft mode.

The matrix $\hat{\mu}(t)$ can be expanded about $t = 0$ for small $|t|$,

$$\hat{\mu}(t) \approx \hat{\mu}(0) + \dot{\hat{\mu}}(0)t, \quad (24)$$

where the time derivative is taken for $t = 0$. This derivative is small, its matrix elements on the eigenvectors $\bar{\mathbf{e}}_\nu(0), \mathbf{e}_{\nu'}(0)$, are $|\dot{\mu}_{\nu\nu'}| \sim \omega_F/t_r^{(0)} \ll (t_r^{(0)})^{-2}$ [here, $\bar{\mathbf{e}}_\nu(0)$ are the left eigenvectors of the matrix $\hat{\mu}(0)$].

With (24), Eq. (22) can be solved for the "fast" components $\delta q_{\nu>1}$. Over a short time $\sim t_r^{(0)}$ they approach their quasistationary values for given δq_1 . Those are small, of order $\delta q_1^2, \delta A, \delta q_1 \omega_F t$, and follow δq_1 adiabatically. Noise-induced fluctuations of $\delta q_{\nu>1}$ about the quasistationary values are also small for small noise intensity. Therefore the effect of $\delta q_{\nu>1}$ on the dynamics of δq_1 can be disregarded.

The equation of motion for δq_1 is of the form

$$\begin{aligned} \dot{\delta q}_1 &= \dot{\mu}_1 t \delta q_1 + \alpha \delta q_1^2 + \beta \delta A + f_1(t), \\ f_1(t) &= \bar{\mathbf{e}}_1(0) \cdot \mathbf{f}(t), \quad \dot{\mu}_1 = \bar{\mathbf{e}}_1(0) \cdot \dot{\hat{\mu}}(0) \mathbf{e}_1(0). \end{aligned} \quad (25)$$

Here, $\alpha = (1/2)(\mathbf{e}_1(0) \cdot \nabla)^2 K_1$, $\beta = \partial K_1 / \partial A$, with $K_1 = \bar{\mathbf{e}}_1(0) \cdot \mathbf{K}$ being now the component of \mathbf{K} in the direction $\mathbf{e}_1(0)$. All derivatives of \mathbf{K} are calculated on the critical cycle $\mathbf{q}_c(t)$ for $t = 0$. Because $|\dot{\mu}_1| \sim \omega_F/t_r^{(0)}$ is small, relaxation of δq_1 is slow compared to relaxation of $\delta q_{\nu>1}$, for typical $|t| \ll \tau_F$.

Eq. (25) describes the stable and unstable states of the original equation of motion (1) in the region $|t| \ll \tau_F$. It is seen that these states, $(\delta q_1)_a$ and $(\delta q_1)_b$, exist provided

$$\dot{\mu}_1 > 0, \quad \alpha \beta \delta A < 0. \quad (26)$$

In this range Eq. (25) is equivalent to Eq. (18). This can be seen if, on the one hand, Eq. (18) is written for the deviation $\delta Q = Q - \tau$ of Q from its value on the critical cycle $Q_c = \tau$, and on the other hand, in Eq. (25) one changes to scaled variables $\delta Q = \alpha(2/\dot{\mu}_1)^{1/2} \delta q_1$ and $\tau = (\dot{\mu}_1/2)^{1/2} t$. The control parameter η in (18) becomes

$$\eta = -2\alpha\beta\dot{\mu}_1^{-1}\delta A. \quad (27)$$

The analysis of Eq. (18) then applies to Eq. (25). In particular, the statement in the beginning of this subsection that the stable and unstable states are at their closest for $t = 0$ is an immediate consequence of the explicit expression for these states (20).

There is an important difference between this approach and the approach of Sec. III B. Because here we do not start from the adiabatic approximation, we formally have not specified how small is the difference between the critical amplitude A_c and its adiabatic value A_c^{ad} . In Eq. (16) we only obtained the linear in $\omega_F t_r^{(0)}$ term in $A_c - A_c^{\text{ad}}$. In general, $A_c - A_c^{\text{ad}}$ has also higher-order terms. They can be obtained by taking into account the dependence of the coefficients α, β, γ in Eq. (B3) on A , which was previously disregarded. This is illustrated for a particular model in Sec. V. It is for the renormalized critical amplitude, i.e., for the control parameter given by Eq. (27), that there holds the exponential limit (21) on the range where the local nonadiabatic approximation applies. The inequality (21) indicates that, for small frequency, the critical amplitude found from the local theory is exponentially close to the exact A_c . This is confirmed by numerical calculations for a model discussed in Sec. V.

IV. ACTIVATION ENERGY OF ESCAPE

It follows from the results of Sec. III that, near a bifurcation point, a periodically driven system has a soft mode Q , and the noise that drives this mode is effectively white. The equation of motion is of the form $dQ/d\tau = G + f(\tau)$ (18), where the function G is given by $G = Q^2 + 1 - \eta - \tau^2$ for $\omega_F t_r \ll 1$ [cf. Eq. (18)] and $G = Q^2 - \eta$ for $\omega_F t_r \gg 1$ [cf. Eq. (23)]. The intensity \tilde{D} of the noise $f(\tau)$ has the form (B7) and (C12) in these two cases.

For a white-noise driven system, the variational problem (9), (10) of calculating the period-averaged rate of activated escape \bar{W} can be written in the form

$$\bar{W} = \text{const} \times \exp(-\tilde{R}/\tilde{D}), \quad \tilde{R} = \min \tilde{\mathcal{R}}[Q], \quad (28)$$

$$\tilde{\mathcal{R}} = \int d\tau L \left(Q, \frac{dQ}{d\tau}, \tau \right), \quad L = \frac{1}{4} \left(\frac{dQ}{d\tau} - G \right)^2.$$

(cf. Appendix A). In contrast to the standard formulation [29], the function G here may depend on time τ and is not time-periodic, in the actual range of τ . The minimization is carried out over the paths $Q(\tau)$ that start at $Q_a(\tau)$ for $\tau \rightarrow -\infty$ and end at $Q_b(\tau)$ for $\tau \rightarrow +\infty$, with time-dependent stable and unstable states $Q_{a,b}(\tau)$. The non-stationarity emerges for slow modulation, where $\omega_F t_r \ll 1$, and is related to the assumptions that (i) escape is most likely to occur during a portion of the period where the states $Q_{a,b}$ are close, and (ii) the duration of motion along the optimal escape path $Q_{\text{opt}}(\tau)$ is much less than the modulation period.

We have solved the variational problem using the Hamilton equations of motion for Q and $P = \partial L / \partial (dQ/d\tau)$,

$$\frac{\partial Q}{\partial \tau} = 2P + G, \quad \frac{\partial P}{\partial \tau} = -P \frac{\partial G}{\partial Q}. \quad (29)$$

We then verified the assumptions made in obtaining Eqs. (28), (29).

Equations (29) were solved numerically. This was done by choosing the initial conditions on the optimal path close to $Q_a(\tau)$ with large but finite negative τ . In this range Eqs. (29) can be linearized in $Q - Q_a(\tau)$. On the solution that goes away from Q_a the momentum P is linear in $Q - Q_a$,

$$P \approx [Q - Q_a(\tau)]/\sigma_a^2(\tau) \quad (30)$$

$$\sigma_a^2(\tau) = 2 \int_{-\infty}^{\tau} d\tau' \exp \left[4 \int_{\tau'}^{\tau} d\tau'' Q_a(\tau'') \right]$$

We used the shooting method: we sought such initial $Q - Q_a(\tau)$ for given τ that the trajectory approaches $Q_b(\tau)$ for large τ , cf. Ref. 18.

Numerical results for the activation energy in the whole range of slow driving, where $\omega_F t_r \ll 1$, are shown below in Figs. 4, 5 on linear and logarithmic scales, respectively. Note that the activation energy is a function of a single control parameter $\eta \propto A_c - A$, and in this sense the results are universal, i.e. system-independent. In the rest of this Section we discuss analytical results and compare them with the numerical results.

A. Activation energy in the adiabatic approximation

The adiabatic regime applies when the driving is slow, $\omega_F t_r \ll 1$, and the system is sufficiently far from the bifurcation point, so that $t_r \ll t_l$ [cf. Eq. (14)] or equivalently $|\delta A^{\text{ad}}| \equiv |A_c^{\text{ad}} - A| \gg \omega_F |\gamma/\beta|$. Respectively, the dimensionless control parameter $\eta \propto A_c - A$ is large, $\eta - 1 \gg 1$, [cf. Eq. (17); we note that the actual parameter in the adiabatic range is not η but $\eta - 1$]. In this case we expect that escape occurs when the adiabatic states (19) are closest to each other, i.e., for $\tau = 0$. Then, in the first approximation, the term τ^2 in the function G in Eq. (18) can be disregarded, and G becomes

$$G^{\text{ad}} = Q^2 + 1 - \eta. \quad (31)$$

The solution of Eq. (29) with G of the form (31) and with boundary conditions $Q(\tau) \rightarrow \mp(\eta - 1)^{1/2}$ for $\tau \rightarrow \mp\infty$ is well known. It is an instanton (kink)

$$Q_{\text{opt}}^{\text{ad}}(\tau, \tau_0) = (\eta - 1)^{1/2} \tanh[(\eta - 1)^{1/2}(\tau - \tau_0)] \quad (32)$$

centered at an arbitrary τ_0 .

The characteristic duration of motion along the path $Q_{\text{opt}}^{\text{ad}}(\tau)$ in dimensionless time is $\Delta\tau \sim (\eta - 1)^{-1/2}$, which corresponds to $\Delta t \sim t_r$ in real time. Since $\Delta\tau \ll (\eta - 1)^{1/2}$, the term τ^2 in the function G [Eq. (18)] can be disregarded compared to $\eta - 1$, which justifies replacing G with G^{ad} as long as $|\tau_0| \ll (\eta - 1)^{1/2}$.

The activation energy (28) calculated along the path $Q_{\text{opt}}^{\text{ad}}$ is

$$\tilde{R}^{\text{ad}} = \frac{4}{3}(\eta - 1)^{3/2} \propto (A_c^{\text{ad}} - A)^{3/2}. \quad (33)$$

This equation shows that the activation energy of escape scales with the distance to the bifurcation point as $(A_c - A)^\xi$ with $\xi = 3/2$ in the adiabatic region.

B. Nonadiabatic correction to the activation energy

We now consider the lowest-order correction to the adiabatic activation energy. Two factors have to be taken into account. First is that, because of the nonzero duration of motion along the escape path $\Delta\tau$, the equilibrium states $Q_{a,b}^{\text{ad}}(\tau)$ change, which was disregarded in the analysis of Sec. IV A. However, the corresponding correction to \tilde{R} is exponentially small. Indeed, if we consider \tilde{R} as a function of the end point Q on the optimal path, we have $|\partial\tilde{R}/\partial Q| = |P|$, where P is the momentum on the optimal path. For an instantonic solution, the momentum goes to zero as $Q_{\text{opt}} \rightarrow Q_{a,b}$, see Eq. (30). Therefore a small change of $Q_{a,b}$ affects the activation energy very weakly.

The major nonadiabatic correction to \tilde{R} comes from the time-dependent term in $G = G^{\text{ad}} - \tau^2$ [cf. Eq. (18)]. This term lifts the time invariance of the instanton $Q_{\text{opt}}(\tau, \tau_0)$ with respect to τ_0 ,

To first order in τ^2 , i.e., to lowest order in $(\eta - 1)^{-2}$, the correction $\delta\tilde{R}$ can be found from Eq. (28) by integrating the term τ^2 along the zeroth order trajectory $Q_{\text{opt}}^{\text{ad}}(\tau, \tau_0)$,

$$\delta\tilde{R} = \min_{\tau_0} \int d\tau' \frac{dQ_{\text{opt}}^{\text{ad}}(\tau', \tau_0)}{d\tau'} \tau'^2. \quad (34)$$

(we used that $dQ_{\text{opt}}^{\text{ad}}/d\tau = -G^{\text{ad}}$). Minimization here is done over τ_0 , the center of the instanton. It is necessary because \tilde{R} is the absolute minimum of the functional $\tilde{\mathcal{R}}$.

A direct calculation shows that the minimum of $\delta\tilde{R}$ is reached for $\tau_0 = 0$, and

$$\delta\tilde{R} = \frac{\pi^2}{6}(\eta - 1)^{-1/2}. \quad (35)$$

The correction $\delta\tilde{R}$ rapidly falls off with increasing $\eta - 1$. On the other hand, as η decreases and becomes ~ 1 , the term $\delta\tilde{R}$ increases very fast, which indicates a breakdown of the adiabatic theory in this region.

The analytical results in the adiabatic region are compared with the numerical solution for the activation energy \tilde{R} in Fig. 4. The corrected adiabatic theory works well in the whole range where the control parameter $\eta \gtrsim 3$, but for smaller η nonadiabatic effects are significant and have to be taken into account in a nonperturbative way.

C. Activation energy in the locally nonadiabatic region

Standard techniques do not allow to solve equations (29) for the optimal path analytically in the general case

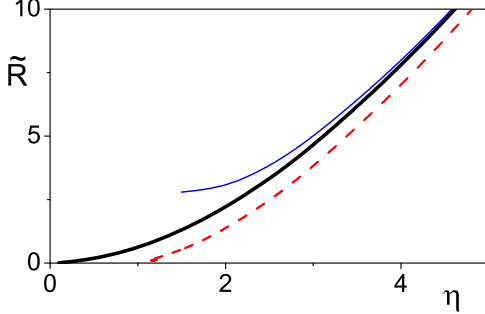


FIG. 4: The activation energy \tilde{R} vs. $\eta \propto A_c - A$ for slow driving, $\omega_F t_r \ll 1$. The thick solid line shows the numerical solution of Eq. (28). The dashed line is the adiabatic activation energy (33), $\tilde{R}^{\text{ad}} \propto (\eta - 1)^{3/2}$. The thin solid line shows the corrected adiabatic activation energy $\tilde{R}^{\text{ad}} + \delta\tilde{R}$. It is close to the numerical result for $\eta \gtrsim 3$. The correction $\delta\tilde{R}$ diverges at the adiabatic bifurcation point $\eta = 1$.

$\eta \sim 1$. This is because the function G in Eq. (29) explicitly depends on time τ . However, a solution can be obtained close to the bifurcation point, where $\eta \propto A_c - A$ is small, but not exponentially small, cf. Eq. (21).

Unusually for an instanton-type problem, and because of the strong time dependence of G , the optimal path can be found by *linearizing* the equations of motion (29) about the critical state $Q_c = \tau$. This gives

$$\delta\dot{Q} = 2\tau\delta Q - \eta + 2P, \quad \dot{P} = -2P\tau, \quad (36)$$

where $\delta Q \equiv Q - \tau$. The solution of these equations with boundary conditions $Q(\tau) \rightarrow Q_{a,b}(\tau)$ for $\tau \rightarrow \mp\infty$ is

$$\begin{aligned} Q_{\text{opt}}(\tau) &= \tau - \eta \int_0^\tau d\tau' [1 - \sqrt{2} e^{-\tau'^2}] e^{\tau^2 - \tau'^2}, \\ P_{\text{opt}}(\tau) &= \eta e^{-\tau^2} / \sqrt{2}, \end{aligned} \quad (37)$$

where we took into account the explicit form of $Q_{a,b}(t)$ (20).

It is seen from Eq. (37) that the momentum on the optimal path P_{opt} has a shape of a Gaussian pulse centered at $\tau = 0$, with width ~ 1 . The coordinate $Q_{\text{opt}}(\tau)$ over the dimensionless time $\tau \sim 1$ switches between the equilibrium states $Q_{a,b}$. The typical duration of motion in real time is t_l .

From Eqs. (37), the nonadiabatic activation energy of escape for $\omega_F t_r \ll 1$ is

$$\tilde{R}^{\text{nonad}} = (\pi/8)^{1/2} \eta^2 \propto (A_c - A)^2. \quad (38)$$

Here, the critical amplitude A_c is given by Eq. (16), to first order in ω_F .

It is seen from Eq. (38) that, in the locally nonadiabatic region, the activation energy again displays scaling behavior, $\tilde{R} \propto (A_c - A)^\xi$. But the scaling exponent is $\xi = 2$, it differs from the adiabatic exponent $\xi = 3/2$

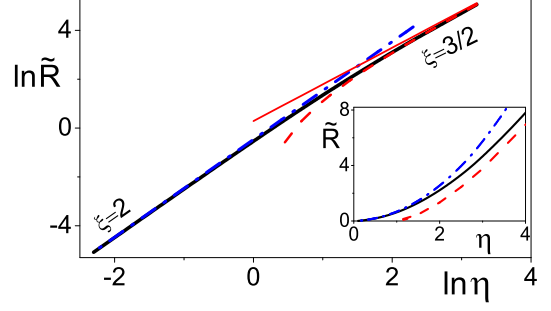


FIG. 5: The activation energy $\tilde{R} = -\tilde{D} \ln \overline{W}$ on a logarithmic and linear scale (inset) vs. $\eta \propto A_c - A$ for slow modulation, $\omega_F t_r \ll 1$. Thick solid lines show the numerical solution of the variational problem (28). It describes the crossover between different scaling regions. The thin solid line shows the adiabatic scaling for large η , $\tilde{R} \propto \eta^{3/2}$. The full result of the adiabatic approximation is shown by the dashed line. The dash-dot line shows the nonadiabatic result (38) that applies for $\eta \ll 1$; here $\tilde{R} \propto \eta^2$.

(33) that has been known for stationary systems. This is a result of the complicated nonadiabatic dynamics associated with avoided crossing of the stable and unstable states. The onset of this scaling behavior is the central result of the paper.

The predicted $\xi = 2$ scaling is compared with the result of the numerical calculation in Fig. 5. The analytical and numerical results are in quantitative agreement in the whole range $\eta \lesssim 2$.

D. Activation energy for $\omega_F t_r \gg 1$

It was shown in Sec. III C that, sufficiently close to a bifurcation point, there holds a condition $\omega_F t_r \gg 1$, even where the modulation frequency is less than the relaxation rate far away from the bifurcation point, $\omega_F t_r^{(0)} \lesssim 1$. Finding the activation energy of escape $\tilde{R} \equiv \tilde{R}^{\text{fast}}$ for $\omega_F t_r \gg 1$ is formally similar to that in the adiabatic approximation. The only difference is that $\eta - 1$ in Eq. (31) should be now replaced by η . This gives

$$\tilde{R}^{\text{fast}} = (4/3)\eta^{3/2} \propto (A_c - A)^{3/2}. \quad (39)$$

Both the coefficient β' that relates η to $A_c - A$ [see Eqs. (23) and (C7)] and the noise intensity \tilde{D} (C12) depend on the arbitrary initial time t_i . It enters the weighting factor $\kappa_{11}(t, t_i)$ which was used in obtaining the equation of motion for the slow variable (23). A straightforward analysis shows that t_i drops out from the ratio $\beta'^{3/2}/\tilde{D}$, which gives the escape rate $\overline{W} \propto \exp(-\tilde{R}^{\text{fast}}/\tilde{D})$.

Eq. (39) shows that the activation energy displays scaling behavior with the distance to the bifurcation point

in the range $\omega_F t_r \gg 1$. The scaling exponent is $\xi = 3/2$, as in the adiabatic case.

E. Scaling crossovers near a critical point

Eqs. (33), (38), and (39) show the onset of three regions where the activation energy of escape displays scaling dependence on the modulation amplitude, $R \propto \tilde{R} \propto (A_c - A)^\xi$. The adiabatic and locally nonadiabatic regions emerge only if the modulation frequency is slow compared to the relaxation rate far from the bifurcation point, $\omega_F t_r^{(0)} \ll 1$. In this case, as seen from Fig. 5, as the bifurcation point is approached, the system displays first the adiabatic scaling $\xi = 3/2$, which for smaller $A_c - A$ goes over into the scaling $\xi = 2$. As the bifurcation point A_c is approached even closer, there emerges the fast-oscillating regime where $\xi = 3/2$ again.

The widths of the regions of different scaling strongly depend on the modulation frequency. For small $\omega_F t_r^{(0)} \ll 1$ the range of amplitudes where motion is effectively fast oscillating, $\omega_F t_r \gg 1$, is exponentially narrow. However this range increases very rapidly with increasing ω_F . The particular way in which the widths of different scaling regions vary with ω_F depends on the system dynamics. Ultimately, for $\omega_F t_r^{(0)} \gtrsim 1$, the regime of effectively fast oscillations becomes the only observable regime near a bifurcation point.

V. SCALING CROSSOVERS FOR A MODEL SYSTEM

To test the occurrence of three scaling regions and the scaling crossovers, we have studied activated escape for a model system, an overdamped Brownian particle in a modulated potential well. It is described by the Langevin equation

$$\begin{aligned} \dot{q} &= -\frac{\partial U(q, t)}{\partial q} + f(t), \quad \langle f(t)f(t') \rangle = 2D\delta(t - t'), \\ U(q, t) &= -\frac{1}{3}q^3 + \frac{1}{4}q - Aq \cos \omega_F t. \end{aligned} \quad (40)$$

The shape of the potential $U(q, t)$ is shown schematically in Fig. 1. In the absence of modulation, $A = 0$, the system has a metastable state at the bottom of the potential well, $q_a = -1/2$, and an unstable equilibrium at the barrier top, $q_b = 1/2$. The relaxation time is $t_r^{(0)} = 1/U''(q_a) = 1$. In the presence of modulation, the states $q_{a,b}$ oscillate in time. As the modulation amplitude A increases to the critical value A_c (the saddle-node bifurcation), the states merge, and then, for $A > A_c$, disappear.

The frequency dependence of the critical amplitude A_c is shown in Fig. 6. In the limit $\omega_F = 0$ we have $A_c \equiv A_c^{\text{ad}} = 1/4$. The linear in ω_F correction to A_c can be obtained from Eq. (16) by noticing that the adiabatic

bifurcational value of the coordinate is $q_c^{\text{ad}} = 0$, and the adiabatic bifurcation occurs for $t = 0$ (or equivalently, $t = n\tau_F$). Near the adiabatic bifurcation point we have

$$\dot{q} = q^2 + \delta A^{\text{ad}} - \frac{1}{2}A\omega_F^2 t^2 + f(t), \quad (41)$$

with $\delta A^{\text{ad}} = A - A_c^{\text{ad}}$. This equation will have the same form as Eq. (12) if we replace the factor A in $A\omega_F^2 t^2$ with $A_c^{\text{ad}} = 1/4$ [as it was done in Eq. (12)].

From Eq. (41) it follows that, for the model under consideration, the parameters in Eq. (12) are $\alpha = \beta = 1$, $\gamma = (A_c^{\text{ad}}/2)^{1/2} = 2^{-3/2}$. Therefore, from Eq. (16), to first order in ω_F the critical amplitude is $A_c^{\text{sl}} = 1/4 + 2^{-3/2}\omega_F$. It is shown in the main part of Fig. 6 with the dashed line.

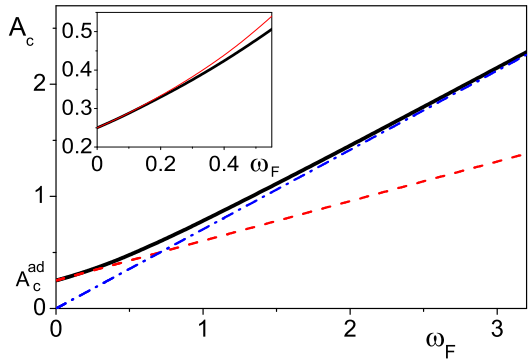


FIG. 6: The critical amplitude A_c as a function of the modulation frequency ω_F for the system (40). Numerical results are shown by thick solid lines. The dashed line shows the linear in ω_F nonadiabatic correction to A_c described by Eq. (16). The thin solid line in the inset describes a correction obtained from the self-consistent local analysis, Eq. (42). The dash-dot line describes the high-frequency asymptotic that follows from Eq. (43).

As discussed in Sec. III D, the local nonadiabatic theory allows us to find higher-order terms in the critical amplitude. This is done by noticing that the critical state $q_c(t)$ into which the stable and unstable states merge at the bifurcation point is linear in t for small t , i.e., $q_c(t) - q_c^{\text{ad}} \propto t$. By substituting this solution into Eq. (41) (without noise) we obtain

$$A_c \approx \left[1 + \omega_F^2 + \omega_F (\omega_F^2 + 2)^{1/2} \right] / 4, \quad \omega_F t_r \ll 1. \quad (42)$$

This equation is in good agreement with the numerical data for $\omega_F t_r^{(0)} \lesssim 0.4$, as seen from the inset in Fig. 6. The difference between the numerical and analytical A_c decreases exponentially fast with decreasing ω_F .

We also evaluated for slow driving the time derivative of the eigenvalue $\mu_1 = 2q_c(t)$ on the critical cycle $q_c(t)$. For the model (41) the stable and unstable states are at their closest for $t = 0$. Eqs. (17), (27) show that, at

this time, $\dot{\mu}_1 = (2A_c)^{1/2}\omega_F$. This value agrees with the numerical values of $\dot{\mu}_1$ to better than 10% for $\omega_F < 0.5$.

In the high frequency limit, $\omega_F t_r^{(0)} \gg 1$, the motion of the system (40) is a superposition of slow motion and fast oscillations at frequency ω_F . To lowest order in ω_F^{-1} we have $q \approx Q + (A/\omega_F) \sin \omega_F t$. The equation for the slow variable Q becomes

$$\dot{Q} = Q^2 - \frac{1}{4} + \frac{A^2}{2\omega_F^2} + f(t). \quad (43)$$

It shows that, for large ω_F , we have $A_c \approx \omega_F/\sqrt{2}$. This is in good agreement with numerical data in Fig. 6 for $\omega_F \gtrsim 2$.

In the intermediate range, $\omega_F t_r^{(0)} \lesssim 1$, the motion may not be separated into slow and fast-oscillating for weak modulation, but the separation becomes possible near a critical point, $\omega_F t_r \gg 1$. Here, the coefficients in the equation of motion for the slow variable and the effective noise intensity (C7), (C12) are nonlocal and had to be evaluated numerically as functions of ω_F .

A. Activation energy

For a periodically modulated overdamped Brownian particle described by Eq. (40), the activation energy of escape R can be found from the variational problem (9), (10) or, equivalently, (28) [18]. The variables Q, P, τ , and the function G in the Lagrangian L (28) and the Hamilton equations (29) should be changed to q, p, t , and $-\partial U(q, t)/\partial q$, respectively. As explained in Sec. II, there is one optimal path per modulation period. The initial condition for the momentum p on the optimal path is

given by Eq. (30), with $Q_a(\tau)$ replaced by $q_a(t)$ [the expression for σ_a^2 can be further simplified taking into account the periodicity of $q_a(t)$]. Then Eqs. (29) can be solved numerically.

The obtained activation energy R as function of the modulation amplitude for four characteristic values of ω_F is shown in Fig. 7. The solid lines on this plot correspond to the results of the numerical solution of the variational problem. The dashed lines in the panels for $\omega_F = 0.1, 0.25$ (we remind that $t_r^{(0)} = 1$) show the adiabatic approximation,

$$R^{\text{ad}} = \min [U(q_b(t)) - U(q_a(t))] = \frac{4}{3} \left(\frac{1}{4} - A \right)^{3/2}.$$

The dash-dot lines on all panels show the locally nonadiabatic approximation near the bifurcation point, which gives

$$R^{\text{nonad}} = \left(\frac{\pi}{8} \right)^{1/2} \left(\frac{2}{\dot{\mu}_1} \right)^{1/2} (A_c - A)^2.$$

In plotting this expression we used the values of A_c and $\dot{\mu}_1$ found numerically (they were very close to the analytical expressions given above).

Finally, the dashed lines in Fig. 7 in the panels for $\omega_F = 0.5, 1$ show scaling for the effectively fast-oscillating regime near the bifurcation point, with

$$R^{\text{fast}} = \frac{4}{3} \beta'^{3/2} \frac{D}{\tilde{D}} (A_c - A)^{3/2}.$$

The coefficients β' and \tilde{D} as given by Eqs. (C7), (C12) were obtained numerically.

It is seen from Fig. 7 that, for small ω_F , the adiabatic approximation applies over a broad region of driving amplitudes. Near the bifurcation point it gives scaling $R \propto (A_c - A)^\xi$ with $\xi = 3/2$ (cf. the panel for $\omega_F = 0.1$). However, close to the bifurcation point this scaling does not work. Instead there emerges the nonadiabatic dynamic scaling with $\xi = 2$. For $\omega_F = 0.1$ the range of the nonadiabatic scaling is comparatively narrow.

As the frequency increases, the amplitude range characterized by the $\xi = 2$ -scaling dramatically increases. For $\omega_F = 0.25$ this is practically the only scaling seen near the bifurcation point.

With further increase of ω_F , close to the bifurcation point there emerges a region of the fast-oscillation scaling $R \propto (A_c - A)^\xi$ where again $\xi = 3/2$. The panel for $\omega_F = 0.5$ shows a crossover from the scaling $\xi = 3/2$ very close to the bifurcation point to the scaling $\xi = 2$ further away from A_c . Note that the frequency $\omega_F = 0.5$ is neither small nor large, and therefore there is a noticeable difference in the coefficients at $(A_c - A)^2$ obtained from

the full variational problem for R and from the locally nonadiabatic theory near the bifurcation point.

When $\omega_F t_r^{(0)} \gtrsim 1$ we do not expect to see scaling for either adiabatic or locally nonadiabatic regime. The only scaling to be expected near the bifurcation point is the fast-oscillation one, with $\xi = 3/2$. This is indeed seen in the panel for $\omega_F = 1$ in Fig. 7. We note that the global fast-oscillation approximation (43) does not apply for $\omega_F t_r^{(0)} = 1$.

B. Simulations

An additional test of the results can be obtained by directly simulating the Brownian dynamics described by Eq. (40). We conducted such simulations using the second order integration scheme of stochastic differential equations developed in Ref. 30. As a result of the simulations we obtained the probability distribution of the

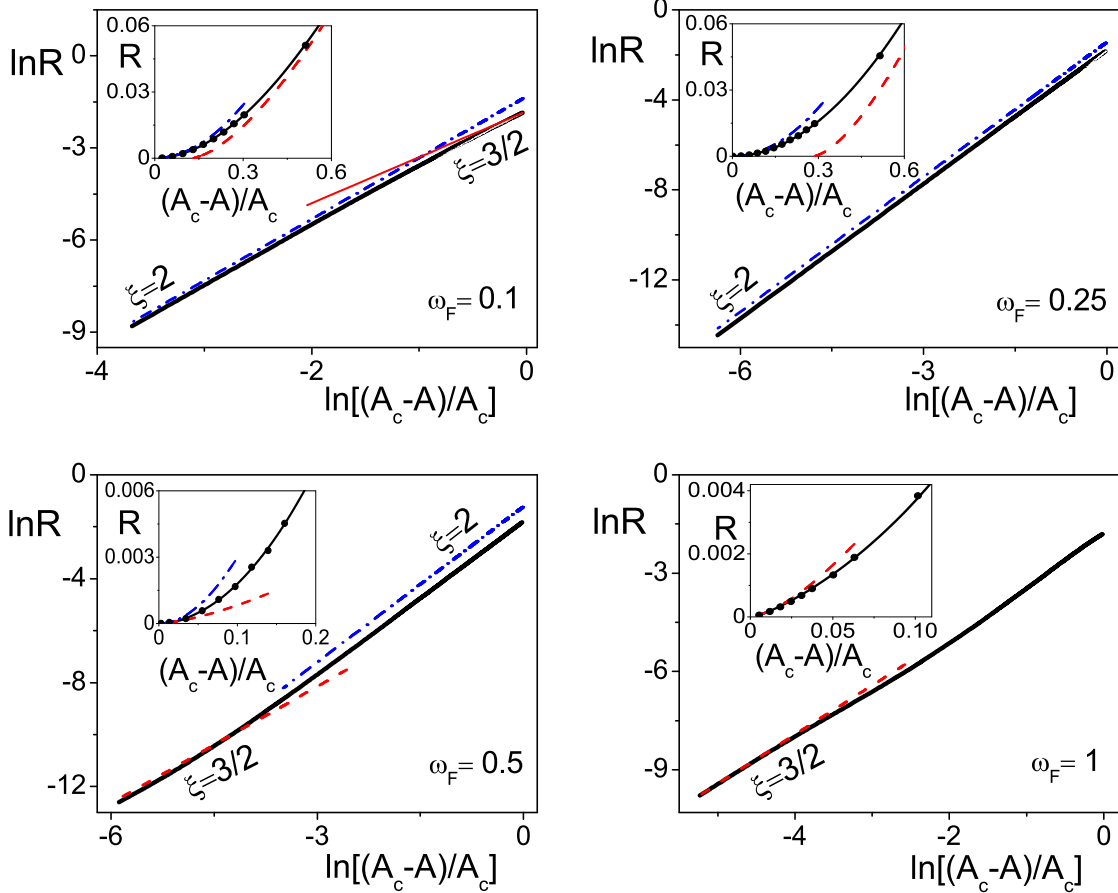


FIG. 7: The activation energy of escape R vs. modulation amplitude A on the logarithmic and linear (inset) scales for a Brownian particle in a modulated potential (40). The values of ω_F are indicated on each panel. The thick solid lines show the results of the numerical solution of the variational problem for R . The dashed lines for $\omega_F = 0.1, 0.25$ show the adiabatic approximation, whereas for $\omega_F = 0.5, 1.0$ they show the approximation of effectively fast oscillations: in the both cases the scaling exponent is $\xi = 3/2$ (for $\omega_F = 0.1$ this asymptotic scaling is shown by the thin solid line). The dash-dot lines show the $\xi = 2$ scaling (38). The dots show the results of numerical simulations of Eq. (40).

dwell time in the metastable state $p_{\text{dw}}(t)$. It gives the probability density (over time) for a system prepared at $t = 0$ close to the attractor to stay in the basin of attraction until time t and leave at that time.

In practice we calculated $p_{\text{dw}}(t)$ by detecting the system at time t at a point q that lied well beyond, but not too far from, the oscillating boundary $q_b(t)$. It is simply related to the time-dependent escape probability $W(t)$, which gives the probability current from the attraction basin at time t if the system was in the stable state at $t = 0$ [15],

$$p_{\text{dw}}(t) = W(t) \exp \left[- \int_0^t dt' W(t') \right]. \quad (44)$$

The average escape rate is given by the mean dwell time,

$$\overline{W} = \left[\int_0^\infty dt t p_{\text{dw}}(t) \right]^{-1}. \quad (45)$$

We studied small noise intensities so that $\overline{W} \ll \omega_F$; then \overline{W} was independent of the position of the ‘‘observation’’ point q .

In most simulations the system was prepared initially at the stable state $q_a(t)$; we found that \overline{W} was independent of the initial state provided it was close to $q_a(t)$.

The dwell-time distribution for a particular set of parameter values in Eq. (40) is shown in Fig. 8. The data refer to modulation at a comparatively low frequency and with comparatively small amplitude. The function $p_{\text{dw}}(t)$ is strongly modulated in time, with period τ_F . This

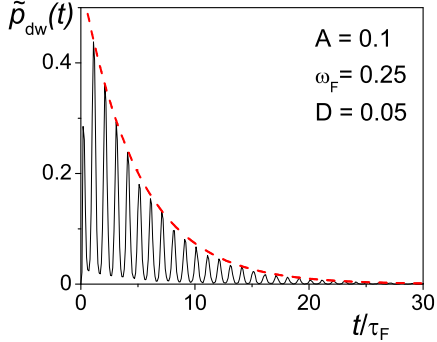


FIG. 8: The scaled probability density of the dwell time $\tilde{p}_{dw}(t) = p_{dw}(t)\tau_F$ obtained by numerical simulations of a Brownian particle in a modulated potential, Eq. (40). The parameters are $A = 0.1$, $D = 0.05$, $\omega_F = 0.25$ (solid line). The dashed line shows the exponential fit of the envelope with decrement $\bar{W}\tau_F = 0.008$.

means that escape events are strongly synchronized by the modulation, in agreement with the analytical results for $W(t)$ obtained for the same model in Ref. 15.

The average escape rate \bar{W} was found from the data of the type shown in Fig. 8 by calculating the mean dwell time (45) and also from an exponential fit of the envelope of $p_{dw}(t)$. These two approaches gave the same result. For each set of A, ω_F, D we observed $\sim 10^5$ escape events. Then D was changed. The activation energy of escape was found from $\ln \bar{W}$ for 2-4 values of D . We tested that it was independent of D in the range $R/D \gtrsim 6$.

The data of simulations are shown in Fig. 7 by dots. For all parameter values they are in excellent agreement with the results of the numerical solution of the variational problem (9).

VI. CONCLUSIONS

In conclusion, we have identified three regions near a bifurcation point where the activation energy of escape displays scaling behavior as a function of the amplitude of periodic modulation. The main results refer to slow modulation, where $\omega_F t_r \ll 1$. We show the emergence of nonadiabatic behavior in this region. The nonadiabaticity leads to a crossover from the scaling with exponent $\xi = 3/2$, previously found for stationary systems, to a new dynamical scaling with $\xi = 2$. The $\xi = 2$ region first emerges near the bifurcation point and then expands with increasing modulation frequency. With further increase of ω_F the crossover $\xi = 2$ to $\xi = 3/2$ can be observed. Again, the effectively fast-oscillating region with $\xi = 3/2$ -scaling emerges first near the bifurcation point. Even though the widths of the regions of different scaling depend on the parameters of a system, the phenomenon of scaling crossovers should be universal.

The onset of the $\xi = 2$ -scaling is a consequence of the slowing down of motion near a bifurcation point. The adiabatic relaxation time of the system t_r strongly depends on the distance to the bifurcation point, $t_r \propto (A_c - A)^{-1/2}$. The nonadiabatic scaling emerges where t_r becomes $\sim [\tau_F t_r^{(0)}]^{1/2}$. For smaller $|A_c - A|$ the dependence of t_r on $A_c - A$ becomes weak, while t_r still largely exceeds the modulation period τ_F . This is associated with avoided crossing of the stable and unstable states, which occurs with decreasing $A_c - A$ as these states are pressed against each other when the system approaches the adiabatic bifurcation point, see Fig. 2.

Both in the adiabatic regime and the nonadiabatic regime for $\omega_F t_r \ll 1$ escape is most likely to occur while the equilibrium states are close to each other. The escape rate is therefore determined by the behavior of the system for a small portion of the modulation period, i.e., locally in time.

The regime of effectively fast oscillations near the bifurcation point emerges for $\omega_F t_r \gg 1$. It can arise even where the modulation period τ_F exceeds the relaxation time far from the bifurcation point. In this regime the motion is controlled by a slow variable, but the dynamics of this variable is no longer determined by local (in time) characteristics. The relevant characteristics are obtained by averaging the appropriate parameters along the critical periodic trajectory of the system into which the stable and unstable periodic cycles merge at the bifurcation point.

We have developed a general formulation of escape of periodically modulated systems driven by colored Gaussian noise. Near a bifurcation point slow motion of the system effectively filters out high-frequency components of the noise spectrum and makes the noise effectively white. From the theoretical point of view it is interesting that, in the locally-nonadiabatic regime of $\xi = 2$ scaling, the instanton-like optimal escape path can be found from linear equations of motion.

We expect that the new $\xi = 2$ scaling and the scaling crossovers can be seen in various systems. Examples are modulated Josephson junctions, nanomagnets, and optically trapped Brownian particles, where escape in the presence of modulation has been already studied experimentally, albeit in different regimes.

This research was supported by the NSF PHY-0071059 and NSF DMR-0305746.

APPENDIX A: VARIATIONAL EQUATIONS FOR THE ESCAPE PROBLEM

We will consider here the optimal trajectory that the system is most likely to follow in escape, $\mathbf{q}_{\text{opt}}(t)$, and the random force $\mathbf{f}_{\text{opt}}(t)$ that drives the system during this motion. The trajectories $\mathbf{q}_{\text{opt}}(t)$, $\mathbf{f}_{\text{opt}}(t)$ provide the absolute minimum to the functional $\mathcal{R}[\mathbf{q}, \mathbf{f}]$ (9). The vari-

ditional equations have the form

$$\int dt' \hat{\mathcal{F}}(t-t') \mathbf{f}(t') - \boldsymbol{\lambda}(t) = 0, \quad (\text{A1})$$

$$\dot{\boldsymbol{\lambda}} = -\nabla(\boldsymbol{\lambda} \cdot \mathbf{K}), \quad (\text{A2})$$

$$\dot{\mathbf{q}} - \mathbf{K}(\mathbf{q}; A, t) - \mathbf{f}(t) = 0 \quad (\text{A3})$$

(here and below we use the hat to indicate a matrix; $\nabla \equiv \partial/\partial \mathbf{q}$).

From Eqs. (7) and (A1) it follows that the optimal noise realization is expressed in terms of the Lagrange multiplier $\boldsymbol{\lambda}$ and the matrix of the noise correlation functions $\hat{\varphi}$ (3) as

$$\mathbf{f}_{\text{opt}} = D^{-1} \int dt' \hat{\varphi}(t-t') \boldsymbol{\lambda}(t'). \quad (\text{A4})$$

Therefore, for the optimal path, the activation energy functional (6) is

$$\mathcal{R} = \frac{1}{2} D^{-1} \iint dt dt' \boldsymbol{\lambda}(t) \cdot \hat{\varphi}(t-t') \boldsymbol{\lambda}(t') \quad (\text{A5})$$

(note that the noise intensity D drops out from \mathcal{R} , because the correlation functions $\varphi_{ij}(t)$ are proportional to the noise intensity themselves).

From the structure of the functional (A5) (integration over time goes from $-\infty$ to ∞ and the integral is non-negative) and from the fact that the system is initially in the vicinity of a stable state one immediately derives the boundary condition (8) for $t \rightarrow -\infty$. The arguments generalize to periodically driven systems the analysis of Ref. 25 for stationary systems.

Close to a periodic stable state $\mathbf{q}_a(t)$ time evolution of $\boldsymbol{\lambda}(t)$ can be described using the matrix $\hat{\mu}_a(t) = (\partial K_i / \partial q_j)_a$, where the derivatives are evaluated for the state $\mathbf{q}_a(t)$. Because of the periodicity of $\mathbf{q}_a(t)$, the matrix $\hat{\mu}_a(t)$ is also periodic in time. It determines the monodromy matrix

$$\hat{M}_a(t) = T_t \exp \left[\int_t^{t+\tau_F} dt_1 \hat{\mu}_a(t_1) \right],$$

where T_t is the operator of chronological ordering (cf. Appendix C). The matrix \hat{M}_a shows how the distance between a point \mathbf{q} and the cycle $\mathbf{q}_a(t)$ varies over the modulation period in the absence of noise for small $|\mathbf{q} - \mathbf{q}_a(t)|$:

$$\mathbf{q}(t + \tau_F) - \mathbf{q}_a(t) = \hat{M}_a(t)[\mathbf{q}(t) - \mathbf{q}_a(t)]$$

From the condition that $\mathbf{q}_a(t)$ is a stable state, the eigenvalues of the matrix \hat{M}_a are all less than 1 in absolute value: in this case the distance between \mathbf{q} and $\mathbf{q}_a(t)$ decreases with increasing time.

It is seen from Eq. (A2) that the monodromy matrix for $\boldsymbol{\lambda}$ is the inverse transposed of \hat{M}_a . Therefore its eigenvalues are all larger than 1 in absolute value. Hence, if

the system is in the stable state $\mathbf{q}_a(t)$ for $t \rightarrow -\infty$, then $\boldsymbol{\lambda}(t) \rightarrow \mathbf{0}$ for $t \rightarrow -\infty$, and from (A1) $\mathbf{f}(t) \rightarrow \mathbf{0}$, too.

For the periodic saddle $\mathbf{q}_b(t)$ on the boundary of the attraction basin, one of the eigenvalues of the corresponding monodromy matrix exceeds 1 in absolute value. It is such a saddle-type boundary that can merge with an attractor at a saddle-node bifurcation we are interested in. Respectively, one eigenvalue of the matrix that describes time evolution of $\boldsymbol{\lambda}$ is < 1 . If $\boldsymbol{\lambda}$ is pointing along the corresponding eigenvector, it will decay as $t \rightarrow \infty$. Then $\mathbf{f}(t)$ will decay, too, from Eq. (A1). This means that the system may asymptotically approach a saddle-type state. Note that there are no optimal paths that would go from one stable state to another, because the condition $\boldsymbol{\lambda} \rightarrow \mathbf{0}$ for $t \rightarrow \infty$ is not satisfied there. This explains the boundary condition (8) for $t \rightarrow \infty$.

Because the function \mathbf{K} is periodic in time, Eqs. (A1)–(A3) with boundary conditions (8) have a periodic set of solutions. If $\mathbf{q}(t), \mathbf{f}(t), \boldsymbol{\lambda}(t)$ is a solution, then $\mathbf{q}(t + \tau_F), \mathbf{f}(t + \tau_F), \boldsymbol{\lambda}(t + \tau_F)$ is a solution, too. These solutions are heteroclinic orbits: they connect the states $\mathbf{q}_a(t), \mathbf{f} = \boldsymbol{\lambda} = \mathbf{0}$ and $\mathbf{q}_b(t), \mathbf{f} = \boldsymbol{\lambda} = \mathbf{0}$, which are also solutions of Eqs. (A1)–(A3). Generally, only one heteroclinic orbit per period provides the minimum to the functional \mathcal{R} (9).

1. Escape in systems with a slow variable

Eqs. (A1)–(A3) are largely simplified if one of the motions in the system is slow and all other variables follow this motion adiabatically, i.e., their relaxation time $t_r^{(0)}$ is much smaller than the relaxation time of the slow variable t_r , at least for a part of the modulation period near a bifurcation point. We will assume that slow motion is described by q_1 ; the variable q_1 itself may be a periodic function modulated by a slowly varying factor Q_1 , as in the case discussed in Sec. III C. In this case we will be interested primarily in the factor Q_1 .

Over a time $\sim t_r^{(0)}$, the variables $q_{i>1}$ reach their equilibrium values $q'_i(q_1, t)$ for given Q_1, t . They are determined by the equations

$$\dot{q}'_i = K_i(q_1, q'_{i>1}; A, t) + f_i \quad (i > 1) \quad (\text{A6})$$

In the absence of noise, $f_i = 0$, the solutions of these equations are periodic for given Q_1 . As we will see below, the terms f_i here are small and give small corrections.

It is important that the periodic solutions $q'_{i>1}$ with $f_{i>1} = 0$ be stable. From this condition and Eq. (A2) it follows immediately that $\lambda_{i>1} = 0$, otherwise the components $\lambda_{i>1}$ would exponentially grow in time, leading to the onset of a large force that would drive the system away from the state (A6) with given Q_1 .

The nonzero component of the Lagrange multiplier λ_1 is determined by the component of the optimal force f_1 . The latter should overcome the restoring force on the slow variable Q_1 and drive it from the stable to the unstable state. But the slowness of Q_1 means that the restoring force is small, and therefore the force f_1 should be

small, too. It is smaller than the force that would be needed to overcome the restoring force for the fast variables by at least a factor $\sim t_r^{(0)}/t_r$. Therefore λ_1 is small as well.

For given $\lambda_1(t)$ we can find all components $f_{i>1}$ from Eq. (A4). They are all $\propto 1/t_r$, and therefore to lowest order in $t_r^{(0)}/t_r$ they can be disregarded in the solution of Eq. (A6) for $q_{i>1}$.

The problem of escape is therefore reduced to a one-dimensional problem for the variable q_1 , the force f_1 , and the Lagrange multiplier λ_1 . In Eq. (A3) for q_1 , the functions $q_{i>1}$ should be replaced by $q'_{i>1}$ calculated for $f_i = 0$.

Further simplification occurs if the noise spectrum is smooth. The analysis here is different for the cases of slow and fast modulation, i.e. whether $\omega_{FT}t_r$ is small or large. The case $\omega_{FT}t_r \gg 1$ is discussed in Appendix C. Here and in Appendix B we consider the case $\omega_{FT}t_r \ll 1$. The major effect of noise on the slow variable q_1 comes from the noise spectral components at frequencies $\omega \lesssim 1/t_r$. If the noise spectrum is flat for such frequencies, the noise can be assumed to be white on the "slow" time scale. In other words, the correlation function $\varphi_{11}(t)$ can be replaced by $2D\delta(t)$ [in this situation it is convenient to choose D from this condition rather than to define it by Eq. (4)]. Then $\mathcal{F}_{11}(t) = \frac{1}{2}\delta(t)$.

For a 1D system driven by white noise of intensity D , Eqs. (A1)–(A3) have a solution

$$\begin{aligned} f_1(t) &= 2\lambda_1(t) = \dot{q}_1 - K_1, \\ \mathcal{R} &= \frac{1}{4} \int dt (\dot{q}_1 - K_1)^2 \end{aligned} \quad (\text{A7})$$

This reduces the variational problem of finding the optimal path to the known formulation for white-noise driven systems [29].

APPENDIX B: REDUCED EQUATION OF MOTION FOR SLOW DRIVING

In this Appendix we derive simplified equations of motion for the case of slow driving where the relaxation time $t_r \ll \tau_F$ and the motion can be described in the adiabatic approximation. We will consider the vicinity of the adiabatic bifurcation point $\mathbf{q} = \mathbf{0}, t = 0, A = A_c^{\text{ad}}$. A convenient basis for \mathbf{q} is provided by the set of the right eigenvectors of the matrix $\hat{\mu} = (\partial K_i / \partial q_j)$, where the derivatives are evaluated at the adiabatic bifurcation point. In this basis the equation of motion (1) has the form

$$\begin{aligned} \dot{q}_i &\approx \mu_i q_i + \frac{1}{2} \sum_{j,k} K_{i;jk} q_j q_k + K_{i;A} \delta A^{\text{ad}} + K_{i;t} t \\ &+ \frac{1}{2} K_{i;tt} t^2 + \sum_j K_{i;jt} q_j t + f_i(t). \end{aligned} \quad (\text{B1})$$

Here $K_{i;jk} = \partial^2 K_i / \partial q_j \partial q_k$, $K_{i;A} = \partial K_i / \partial A$, etc, with all derivatives calculated at the adiabatic bifurcation point,

and $\delta A^{\text{ad}} = A - A_c^{\text{ad}}$. Since the function \mathbf{K} depends on t only in terms of the modulation phase $\phi = \omega_{FT}t$, we have $K_{i;t} \propto \omega_{FT}$. The expansion in t in (B1) is, in fact, an expansion in $\omega_{FT}t$.

Because the eigenvalue μ_1 is equal to zero, for small $|\mathbf{q}|$ relaxation of q_1 is much slower than relaxation of $q_{i>1}$. In the absence of noise, over the relaxation time $t_r^{(0)}$ the variables $q_{i>1}$ approach their quasistationary values for given q_1 and $\phi = \omega_{FT}t$. They can be obtained from the equations of motion (B1) for $q_{i>1}$ in which \dot{q}_i and $f_i(t)$ are disregarded,

$$q_i \approx -\mu_i^{-1} [K_{i;t} t + K_{i;11} q_1^2 + K_{i;A} \delta A^{\text{ad}} + \dots] \quad (i > 1). \quad (\text{B2})$$

Here, the major term is linear in $\omega_{FT}t$. The full expression is a series in $q_1, \omega_{FT}t$, and δA , and the omitted terms are of higher order in these variables. Because of the noise, $q_{i>1}$ will additionally perform small fluctuations with amplitude $\propto D^{1/2}$.

The dynamics of the slow variable q_1 on times exceeding $t_r^{(0)}$ is given by Eq. (B1) with $i = 1$, in which $q_{i>1}$ are replaced with their quasistationary values. To lowest order in q_1 , δA^{ad} , and $\omega_{FT}t$ only the linear in t term should be kept in Eq. (B2). This gives

$$\begin{aligned} \dot{q}_1 &= \alpha q_1^2 + \beta \delta A^{\text{ad}} - \alpha \gamma^2 (\omega_{FT}t)^2 + f_1(t), \\ \alpha &= \frac{1}{2} K_{1;11}, \quad \beta = K_{1;A}, \end{aligned} \quad (\text{B3})$$

with

$$\begin{aligned} \gamma^2 &= -K_{1;11}^{-1} \omega_{FT}^{-2} \left(K_{1;tt} + \sum_{i,j>1} \mu_i^{-1} \mu_j^{-1} K_{1;ij} K_{i;t} K_{j;t} \right. \\ &\quad \left. - 2 \sum_{j>1} \mu_j^{-1} K_{1;jt} K_{j;t} \right). \end{aligned} \quad (\text{B4})$$

Note that the coefficient γ is independent of ω_{FT} .

Eq. (B3) reduces the multi-dimensional problem of random motion near a bifurcation point to a one-dimensional problem. In the case of a one-dimensional overdamped system driven by an additive periodic force it was derived earlier in Refs. 31, 32. Besides the noise term, it differs from the equation of motion for stationary systems in the vicinity of a saddle-node bifurcation point [11] in that it has a term $\propto (\omega_{FT}t)^2$.

Depending on the sign of δA^{ad} , Eq. (B3) has either two adiabatic solutions

$$(q_1)_{a,b}^{\text{ad}} = \mp \text{sgn}(\alpha) [-(\beta/\alpha) \delta A^{\text{ad}} + (\gamma \omega_{FT}t)^2]^{1/2} \quad (\text{B5})$$

or none. For concreteness, we assume that the adiabatic solutions exist for $\delta A^{\text{ad}} < 0$, i.e. $\alpha\beta > 0$. The solutions are even functions of time. They touch each other at $t = 0$ for $\delta A^{\text{ad}} = 0$. We assume that the periodic adiabatic states $\mathbf{q}_{a,b}^{\text{ad}}(t)$ exist for all times provided $\delta A^{\text{ad}} < 0$.

The term $K_{1;t} t$ in Eq. (B1) has to be equal to zero, otherwise the bifurcation point will be far from $\delta A^{\text{ad}} = t = 0$. On the other hand, the equation of motion (B3) may contain the term $C q_1 \omega_{FT} t$, where C is a sum of $K_{1;1t}$ and appropriately weighted products $K_{1;1i} K_{i;t}$.

This term can be eliminated by a linear transformation $q_1 \rightarrow q_1 + C\omega_F t/2\alpha$ and renormalizations $\delta A^{\text{ad}} \rightarrow \delta A^{\text{ad}} + C\omega_F/2\alpha\beta$, $\gamma^2 \rightarrow \gamma^2 + (C/2\alpha)^2$. The renormalized γ^2 should be positive, if the stable and unstable adiabatic periodic states touch each other only for $\delta A^{\text{ad}} = t = 0$ and only once per period.

The term $\propto q_1 \omega_F t$ does not arise in the important case where the modulation is performed by an additive periodic force $\mathbf{F}(t)$, see Eq. (2). Here, the adiabatic states $\mathbf{q}_{a,b}^{\text{ad}}(t)$ correspond to the minimum and maximum of the potential $U_0(\mathbf{q}) - \mathbf{F}(t) \cdot \mathbf{q}$, cf. Fig. 1. They merge first with increasing modulation amplitude A when the field component $|F_1|$ is at its maximum over t . This means that $\partial_t \mathbf{K} = \partial_{\mathbf{q}} \partial_t \mathbf{K} = \mathbf{0}$ at the bifurcation point.

As explained in Sec. III, the typical relaxation time near the bifurcation point does not exceed $t_l = (\alpha\gamma\omega_F)^{-1/2}$. If the correlation time of the noise $f_1(t)$ is much less than t_l, t_r^{ad} and the power spectrum of the noise does not have singular features for high frequencies, then the dimensionless noise

$$\tilde{f}(\tau) \equiv (\gamma\omega_F)^{-1} f_1(t) \quad (\tau = t/t_l) \quad (\text{B6})$$

is effectively δ -correlated as a function of the “slow” time τ , with $\langle \tilde{f}(\tau) \tilde{f}(0) \rangle = 2\tilde{D}\delta(\tau)$. From Eqs. (3), (B6) the effective noise intensity is

$$\tilde{D} = |\alpha/4|^{1/2} (\gamma\omega_F)^{-3/2} \int_{-\infty}^{\infty} dt \varphi_{11}(t). \quad (\text{B7})$$

APPENDIX C: REDUCED EQUATION OF MOTION FOR FAST DRIVING

In this Section we consider the case where modulation near the bifurcation point is effectively fast, so that $\omega_F t_r \gg 1$. Here, throughout the modulation cycle the stable and unstable states $\mathbf{q}_{a,b}(t)$ stay close to each other and to the critical cycle $\mathbf{q}_c(t)$ into which they merge at the bifurcation point $A = A_c$. Therefore the equation of motion (1) can be expanded in $\delta \mathbf{q} = \mathbf{q} - \mathbf{q}_c(t)$, $A - A_c$, leading to Eq. (22). The expansion coefficients are periodic in time.

It is convenient to start the analysis by simplifying the part of Eq. (22)

$$\delta \dot{\mathbf{q}} = \hat{\mu} \delta \mathbf{q}, \quad \hat{\mu} = \hat{\mu}(t + \tau_F),$$

that describes motion in the linear approximation in $\delta \mathbf{q}$. We introduce the matrix $\hat{\kappa}(t, t_i)$ such that

$$\hat{\kappa}(t, t_i) = T_t \exp \left(\int_{t_i}^t dt_1 \hat{\mu}(t_1) \right), \quad (\text{C1})$$

where T_t is the operator of chronological ordering. This matrix satisfies the equation $\partial \hat{\kappa}(t, t_i) / \partial t = \hat{\mu}(t) \hat{\kappa}(t, t_i)$ and gives the monodromy matrix \hat{M} ,

$$\hat{M}(t) \equiv \hat{M}(t + \tau_F) = \hat{\kappa}(t + \tau_F, t).$$

The eigenvalues M_ν of the matrix \hat{M} determine the evolution of $\delta \mathbf{q}(t)$ in linear approximation. Over the period τ_F , the coefficients of the expansion of $\delta \mathbf{q}(t)$ in the right eigenvectors $\mathbf{e}_\nu(t)$ of \hat{M} change in M_ν times (we use Greek letters to enumerate eigenvalues and eigenvectors; they should be distinguished from the vector components, like q_i). The eigenvalues M_ν are independent of time because of periodicity of $\hat{M}(t), \hat{\mu}(t)$. They are simply related to the Floquet exponents for the periodic state $\mathbf{q}_c(t)$.

At the saddle-node bifurcation, where stable and saddle-type states coalesce, one of the eigenvalues (for example, M_1) becomes equal to 1, whereas $|M_{\nu>1}| < 1$. This means that the system is attracted to $\mathbf{q}_c(t)$ in all directions except for the critical direction $\mathbf{e}_1(t)$; the distance from $\mathbf{q}_c(t)$ along $\mathbf{e}_1(t)$ does not change over the period, in linear approximation. In what follows we choose \mathbf{e}_1 to be real.

For small δA of an appropriate sign, the state $\mathbf{q}_c(t)$ splits along $\mathbf{e}_1(t)$ into a stable and an unstable state. The system approaches the vicinity of these states along the directions $\mathbf{e}_{\nu>1}$ over a short time $\tau_F \max [1/|\ln |M_{\nu>1}||] \sim t_r^{(0)}$. In contrast, the motion along \mathbf{e}_1 is slow.

The \mathbf{e}_1 -component of $\delta \mathbf{q}$ is the soft mode. We are interested in its dynamics on times long compared to $t_r^{(0)}, \tau_F$. The analysis is simplified by the fact that, for $t - t_i \gg |\tau_F / \ln |M_{\nu>1}||$, the matrix $\hat{\kappa}(t, t_i)$ projects any vector $\delta \mathbf{q}(t_i)$ on the vector $\mathbf{e}_1(t)$. In particular,

$$\hat{\kappa}(t, t_i) \mathbf{e}_1(t_i) \approx \kappa_{11}(t, t_i) \mathbf{e}_1(t). \quad (\text{C2})$$

This is a consequence of the transitive property $\hat{\kappa}(t, t_i) = \hat{\kappa}(t, t') \hat{\kappa}(t', t_i)$ and the fact that, for an arbitrary vector $\delta \mathbf{q}$, we have $\hat{M}^n(t) \delta \mathbf{q} \rightarrow C \mathbf{e}_1(t)$ for $n \rightarrow \infty$. The function κ_{11} in Eq. (C2) is given by the expression

$$\kappa_{11}(t, t_i) = \bar{\mathbf{e}}_1(t) \cdot \hat{\kappa}(t, t_i) \mathbf{e}_1(t_i).$$

Here, $\bar{\mathbf{e}}_1$ is the left eigenvector of the matrix \hat{M} , which corresponds to the eigenvalue $M_1 = 1$, and we use normalization $\bar{\mathbf{e}}_1(t) \cdot \mathbf{e}_1(t) = 1$. The matrix element $\kappa_{11}(t, t_i)$ is periodic, $\kappa_{11}(t + \tau_F, t_i) = \kappa_{11}(t, t_i)$.

Equation of motion for $\kappa_{11}(t, t_i)$ for large $t - t_i$ follows from Eq. (C1),

$$\begin{aligned} \frac{\partial}{\partial t} [\kappa_{11}(t, t_i) \mathbf{e}_1(t)] &= \mu_{11}(t) \kappa_{11}(t, t_i) \mathbf{e}_1(t), \\ \mu_{11}(t) &= \bar{\mathbf{e}}_1(t) \cdot \hat{\mu}(t) \mathbf{e}_1(t). \end{aligned} \quad (\text{C3})$$

Close to the bifurcation point, the component of $\delta \mathbf{q}$ along the vector $\mathbf{e}_1(t)$ has a slowly varying factor. In contrast, the components of $\delta \mathbf{q}$ along the vectors $\mathbf{e}_{\nu>1}$ are “fast”. Over time $\gtrsim t_r^{(0)}$ they reach quasiperiodic values for a given value of the slow component, and then fluctuate with amplitude $\propto D^{1/2}$. From (22), the quasiperiodic values are quadratic in the slow component and therefore

small. As a consequence, the slow motion is indeed one-dimensional,

$$\delta\mathbf{q}(t) \approx Q_1(t)\kappa_{11}(t, t_i)\mathbf{e}_1(t). \quad (\text{C4})$$

The instant t_i here is arbitrary; $Q_1(t)$ contains a multiplicative factor that depends on t_i (but $\delta\mathbf{q}(t)$ is independent of t_i). The time t_i drops out of all final expressions, see Sec. IV.

The equation for $Q_1(t)$ is obtained by substituting Eq. (C4) into Eq. (22) and then multiplying Eq. (22) by the vector $\bar{\mathbf{e}}_1(t)$ from the left. This gives

$$\begin{aligned} \kappa_{11}(t, t_i)\dot{Q}_1 &= \mathcal{K}(Q_1, t) + \bar{\mathbf{e}}_1(t) \cdot \mathbf{f}(t), \\ \mathcal{K}(Q_1, t) &= \frac{1}{2}\kappa_{11}^2(t, t_i)Q_1^2(\mathbf{e}_1(t) \cdot \nabla)^2K_1 + \delta A(\partial_A K_1), \end{aligned} \quad (\text{C5})$$

where $K_1 = \bar{\mathbf{e}}_1 \cdot \mathbf{K}$.

In the absence of noise, the solution of Eq. (C5) is a sum of smooth and oscillating parts, $Q_1(t) = Q^{\text{sm}}(t) + Q^{\text{osc}}$. The term Q^{sm} remains nearly constant on the time scale τ_F , whereas $\dot{Q}^{\text{osc}} \sim \omega_F Q^{\text{osc}}$. It is seen from Eq. (C5) that $Q^{\text{osc}} \propto \delta A$. The term Q^{sm} is much larger. An equation for Q^{sm} can be obtained by averaging Eq. (C5) over time. It has the form

$$\dot{Q}^{\text{sm}} = \alpha'(Q^{\text{sm}})^2 + \beta'\delta A + f'(t). \quad (\text{C6})$$

The coefficients α', β' in Eq. (C6) are given by the expressions

$$\begin{aligned} \alpha' &= \frac{1}{2}\langle\kappa_{11}(t, t_i)(\mathbf{e}_1(t) \cdot \nabla)^2K_1\rangle_t, \\ \beta' &= \langle\kappa_{11}^{-1}(t, t_i)\partial K_1/\partial A\rangle_t, \end{aligned} \quad (\text{C7})$$

where $\langle \cdot \rangle_t$ means period-average centered at time t ,

$$\langle \mathcal{G} \rangle_t = \tau_F^{-1} \int_{t-\tau_F/2}^{t+\tau_F/2} dt' \mathcal{G}(t', t_i). \quad (\text{C8})$$

The result of the averaging (C8) is independent of t for time-periodic \mathcal{G} , as in the case of the coefficients α', β' , and therefore α', β' are independent of t .

The function $f'(t)$ in Eq. (C6) is a random force,

$$f'(t) = \kappa_{11}^{-1}(t, t_i)\bar{\mathbf{e}}_1(t) \cdot \mathbf{f}(t). \quad (\text{C9})$$

Eq. (C6) has the same form as the equation for the soft mode in the adiabatic limit (12) in the absence of the term $\propto (\omega_F t)^2$. For $\alpha'\beta' \delta A < 0$ the system has a stable and an unstable stationary solution $Q_{a,b}^{\text{sm}}$. These solutions are given by an equation similar to Eq. (19),

$$Q_{a,b}^{\text{sm}} = \mp \text{sgn}(\alpha')(-\beta' \delta A/\alpha')^{1/2} \quad (\text{C10})$$

(in what follows without lost of generality we set $\alpha' > 0$).

Typical values of Q^{sm} are $\propto |\delta A|^{1/2}$, as seen from Eq. (C10). They largely exceed the amplitude of the fast variables in $\delta\mathbf{q}$, which are all $\propto \delta A$, in the neglect of noise. The relaxation time of Q^{sm} is $t_r = |2\alpha Q_a^{\text{sm}}|^{-1} \propto |\delta A|^{-1/2}$. It is much larger than τ_F close to the bifurcation point. The condition $\omega_F t_r \gg 1$ was the major approximation made in the derivation of Eqs. (C5), (C6), besides the condition of the weak noise.

A transformation from Q^{sm}, t to reduced variables

$$Q = \alpha'^{1/2}Q^{\text{sm}}, \quad \tau = \alpha'^{1/2}t \quad (\text{C11})$$

allows us to write Eq. (C6) in the compact form (23). The random force $\tilde{f}(\tau) = f'(\alpha'^{1/2}t)$ is effectively δ -correlated. From Eqs. (3), (C9), its intensity is

$$\begin{aligned} \tilde{D} &= |\alpha'/4|^{1/2} \int_{-\infty}^{\infty} dt_1 \langle \kappa_{11}^{-1}(t+t_1, t_i)\kappa_{11}^{-1}(t+t_2, t_i) \\ &\quad \times \bar{\mathbf{e}}_1(t+t_1) \cdot \hat{\varphi}(t_1 - t_2)\bar{\mathbf{e}}_1(t+t_2) \rangle_t. \end{aligned} \quad (\text{C12})$$

Here, $\hat{\varphi}$ is the matrix of the noise correlation functions (3).

As a result of the period-averaging over t , in Eq. (C12) the integrand becomes a function of $t_1 - t_2$, and therefore the integral over t_1 is independent of t_2 . Still, it depends on t_i , but this dependence will drop out of the final expressions for observable quantities, in particular the activation energy of escape.

[1] J. Kurkijärvi, Phys. Rev. B **6**, 832-835 (1972).
[2] T.A. Fulton and L.N. Dunkelberger, Phys. Rev. B **9**, 4760-4768 (1974).
[3] J.M. Martinis, M.H. Devoret, and J. Clarke, Phys. Rev. B **35**, 4682-4698 (1987).
[4] F. Sharifi *et al.*, Phys. Rev. Lett. **61**, 742-745 (1988).
[5] S. Han, J. Lapointe, and J. E. Lukens, Phys. Rev. Lett. **63**, 1712-15 (1989); Y. Yu *et al.*, Science **296**, 889 (2002).
[6] W. Wernsdorfer, E.B. Orozco, K. Hasselbach, A. Benoit, B. Barbara, N. Demonyc, A. Loiseau, H. Pascard, and D. Mailly, Phys. Rev. Lett. **78**, 1791 (1997); W.T. Coffey, D.S.F. Crothers, J.L. Dormann, Yu.P. Kalmykov, E.C. Kennedy, and W. Wernsdorfer, Phys. Rev. Lett. **80**, 5655 (1998).
[7] R.H. Koch, , G. Grinstein, G.A. Keefe, Yu Lu, P.L. Trouilloud, and W.J. Gallagher, Phys. Rev. Lett. **84**, 5419 (2000); J.Z. Sun *et al.*, Appl. Phys. Lett. **78**, 4004 (2001).
[8] E. B. Myers, , F. J. Albert, J. C. Sankey, E. Bonet, R. A. Buhrman, and D. C. Ralph, Phys. Rev. Lett. **89**, 196801 (2002).
[9] The $\eta^{3/2}$ behavior near a termination point $\eta_c = 0$ of a metastable state describes the vanishing of the mean-field free-energy barrier with the control parameter η [L.D. Landau and E.M. Lifshitz, *Statistical Physics*, pt. 1, 3rd edition revised by E.M. Lifshitz and L.P. Pitaevskii

(Pergamon, Oxford 1980). This behavior was discussed in various contexts, such as Josephson junctions [1] and magnets [R.H. Victora, Phys. Rev. Lett. **63**, 457 (1989)], as well as nonequilibrium fluctuating dynamical systems [M.I. Dykman and M.A. Krivoglaz, Physica A **104**, 480 (1980); R. Graham and T. Tél, Phys. Rev. A **35**, 1328 (1987)], chemical systems [M.I. Dykman, E. Mori, J. Ross, and P. Hunt, J. Chem. Phys. **100**, pp. 5735 - 50 (1994)], and resonant tunneling structures [O.A. Tretiakov, T. Gramespacher, and K.A. Matveev, Phys. Rev. B **67**, 073303 (2003)].

[10] Scaling with noise intensity for a parameter drifting through an indeterminate saddle-node bifurcation was considered by R. Breban, H.E. Nusse, and E. Ott, nlin.CD/0303059.

[11] J. Guckenheimer and P. Holmes, *Nonlinear Oscillators, Dynamical Systems and Bifurcations of Vector Fields* (Springer-Verlag, NY 1987); V. Arnold, *Ordinary Differential Equations*, 3rd ed. (Springer, New York 1992).

[12] A.I. Larkin and Yu.N. Ovchinnikov, J. Low Temp. Phys. **63**, 317 (1986); B.I. Ivlev and V.I. Mel'nikov, Phys. Lett. A **116**, 427 (1986); S. Linkwitz and H. Grabert, Phys. Rev. B **44** 11888, 11901 (1991).

[13] M.H. Devoret, D. Esteve, J.M. Martinis, A. Cleland, and J. Clarke, Phys. Rev. B **36**, 58-73 (1987). E. Turlot, S. Linkwitz, D. Esteve, C. Urbina, M.H. Devoret, and H. Grabert, Chem. Phys. **235**, 47 (1998).

[14] I. Dayan, M. Gitterman, and G. H. Weiss, Phys. Rev. A **46**, 757 (1992); R. N. Mantegna and B. Spagnolo, Phys. Rev. Lett. **76**, 563 (1996).

[15] V.N. Smelyanskiy, M.I. Dykman, and B. Golding, Phys. Rev. Lett. **82**, 3193 (1999).

[16] J. Lehman, P. Riemann, and P. Hänggi, Phys. Rev. Lett. **84**, 1639 (2000).

[17] R.S. Maier and D.L. Stein, Phys. Rev. Lett. **86**, 3942 (2001).

[18] M.I. Dykman, B. Golding, L.I. McCann, V. N. Smelyanskiy, D. G. Luchinsky, R. Mannella, and P. V. E. McClintock, Chaos **11**, 587 (2001) and references therein.

[19] S.M. Soskin, R. Mannella, and P.V.E. McClintock, Phys. Rep. **373**, 247 (2003)

[20] M.V. Fistul, A. Wallraff, and A.V. Ustinov, cond-mat/0307668.

[21] M.I. Dykman, D.G. Luchinsky, R. Mannella, P.V.E. McClintock, N.D. Stein, and N.G. Stocks, Nuovo Cimento D **17**, 661 (1995).

[22] K. Wiesenfeld and F. Jaramillo, Chaos **8**, 539 (1998).

[23] F. Jülicher, A. Ajdari, and J. Prost, Rev. Mod. Phys. **69**, 1269 (1997); P. Riemann, Phys. Rep. **361**, 57 (2002).

[24] Optimal fluctuational trajectories for white-noise driven systems were first studied by L. Onsager and S. Machlup, Phys. Rev. **91**, 1505-15 (1953), and A.D. Ventcel' and M.I. Freidlin, Russian Math. Surveys **25**, 1 (1970).

[25] M.I. Dykman, Phys. Rev. A **42**, 2020 (1990).

[26] R.P. Feynman, A.R. Hibbs, *Quantum Mechanics and Path Integrals* (McGraw-Hill, New York, 1965).

[27] J.S. Langer, Ann. Phys. **41**, 108 (1967); S. Coleman, Phys. Rev. D **15**, 2929 (1977).

[28] L.D. Landau and E.M. Lifshitz *Mechanics* (Pergamon, London 1976).

[29] M. I. Freidlin and A. D. Wentzel, *Random Perturbations in Dynamical Systems* (Springer, New-York, 1984).

[30] R. Mannella, Intern. J. Mod. Phys. C **13**, 1177 (2002)

[31] N. Berglund and B. Gentz, J. Phys. A **35**, 2057 (2002).

[32] M.I. Dykman, B. Golding, J.R. Kruse, L.I. McCann, D. Ryvkine, cond-mat/0204621